Characterization of Bubble Column Using Electrical Resistance Tomography and Image Processing

Chaitanya Vudikala

A Dissertation Submitted to
Indian Institute of Technology Hyderabad
In Partial Fulfillment of the Requirements for
The Degree of Master of Technology

भारतीय प्रौद्योगिकी संस्थान हैदराबाद
Indian Institute of Technology Hyderabad

Department of Chemical Engineering

June, 2014

Declaration

I declare that this written submission represents my ideas in my own words, and where others' ideas or words have been included, I have adequately cited and referenced the original sources. I also declare that I have adhered to all principles of academic honesty and integrity and have not misrepresented or fabricated or falsified any idea/data/fact/source in my submission. I understand that any violation of the above will be a cause for disciplinary action by the Institute and can also evoke penal action from the sources that have thus not been properly cited, or from whom proper permission has not been taken when needed.

Chaitanya V

Roll No: CH12M1019

ii

Approval Sheet

This thesis entitled "Characterization of Bubble Column Using Electrical Resistance Tomography and Image Processing" by Chaitanya Vudikala (CH12M1019) is approved for the degree of Master of Technology from IIT Hyderabad, July, 2014.

Dr. Narasimha Mangadoddy; Asst. Professor
Adviser

Dr. Vinod Janardhanan; Associate Professor
Examiner

Dr. Aubrey Maiza; Associate Professor
University of Cape Town, External Examiner

Acknowledgements

I express my gratitude to my supervisor Dr. Narasimha Mangadoddy for his excellent guidance and support throughout my M.Tech project.

I would like to thank my thesis committee members Dr. Dayadeep Monder, Dr. Raja Banerjee, and Dr. Vinod Janardhanan for their encouragement, intuitive comments, and valuable suggestions. I would also like to express my thanks to Director Uday B. Desai.

I would like to show my deep appreciation to my lab mates Rakesh Arugonda, Balaraju Vadlakonda, Teja Reddy Vakamalla, Ravi K Gujjula and Mayank Kumar for their co-operation and help.

I would also like to thank my friends Anil Rajapantulu, Srikanth Kutla, Santosh Kumar Varanasi, Swarnalatha Mailaram and Siva Prasad Reddy for helping me in performing experiments and coding.

I would like to express my greatest gratitude to my parents, and my siblings for their encouragement and support throughout my life. My sincere thanks to all the people who helped and supported me during the course of this M.Tech program at Indian Institute of Technology, Hyderabad.

Last but not least, I would like to thank my dear friends and classmates for helping me through the depths of despair.

Dedicated to

My Mother

Abstract

Bubble columns are widely used a gas-liquid contactors in industrial processes for carrying out gas-liquid two phase and gas-liquid-solid three phase contacting operation in the areas of chemical, petrochemical, biochemical and environmental engineering applications. There are many techniques available to measure the characteristics of the flow in the bubble column.Electrical tomography (ERT, ,ECT and EIT), PIV, X-Ray tomography and the gamma ray tomography are some of the techniques used to measure the internal flow dynamics non intrusively.

A high speed dual plane electrical resistance tomography (ERT) system and high speed video camera were applied to a bubble column for the estimation of time averaged gas hold-up and bubble size distribution (BSD) respectively.

An ERT system gives the images based on the internal conductivity distribution of a bubble column content from the measured boundary voltages of. Although ERT is attractive in terms of its much higher scanning rate, but the key challenge is to obtain enough accurate definition of phase boundaries. Using a dual-plane high speed ERT system, measurement of two phase distributions are examined. The experiments are carried out in a 4 inch inner diameter and thickness of 5 mm bubble column. The results are presented in terms of the gas-holdup and bubble size distribution for various gas flow rates and for different spargers. The tomographic images were created through modified sensitivity back projection algorithm and compared with other improved reconstruction algorithms. It is confirmed by ERT that the gas-holdup increases with increasing the air flow rate. In order to compare the reliability of ERT measurements, a high speed video camera was used to get bubble size distribution from where we can calculate the average gas holdup. Bubble characteristics such as shape, size, count and motion were analyzed using an image analysis method.

It has been observed that bubble size distribution is more at central region of bubble column and gas holdup value increases with the increase of gas feed flowrate. Almost the same trend was observed with the ERT data obtained and percentage of error was estimated as 36.146 % for 1mm sparger.

Nomenclature

€	Gas Holdup
$\boldsymbol{\sigma}$	Conductivity
j	Current density
u	Electric potential
E	Electric field
ρ	Resistivity
J	Jacobian
J^T	Transpose of Jacobian
e_l	electrode area
U	vector of nodal voltages
I_l	vector of injected currents
V_l	vector of electrode voltages

Abbreviations

ERT	Electrical Resistance tomography
DAS	Data acquisition system
EIT	Electrical impedance tomography
TV	Total variation
GN	Guass Newton
LBP	Linear back projection
PIV	Particle image velocimetry
CFD	Computational fluid dynamics
AC	Alternate current
IRA	Image reconstruction algorithm
ITS	Industrial tomography system
HSVC	High speed video camera
ECT	Electrical Capacitance tomography

List of Figures

Contents

Chapter 1

Introduction

1.1) Background:

Bubble columns are devices in which gas, in the form of bubbles, comes in contact with liquid. They are widely used due to their ease of operation and ability to enable good gas/liquid mixing and high heat transfer rates in a controlled manner [2][5]. These are widely used in industrial processes for carrying out gas-liquid two phase and gas-liquid-solid three phase contacting operation in the areas of chemical, petrochemical, biochemical and environmental engineering applications, such as petroleum refining, hydrogenation, oxidation, chlorination, crystallization, fermentation, coal treatment, gas absorption, wastewater treatment and production of methanol or other environmental alternative fuels etc.[1][18]

Bubble column construction is of vertically arranged cylindrical column as shown in figure 1. Gas is introduced at the bottom of the column with the help of a sparger and causes a turbulent stream to enable optimum gas-liquid mixing. It requires less energy than mechanical stirring. The liquid can be in co-current flow or in counter-current. The gas is dispersed to create small bubbles and distribute them uniformly over the cross section of the equipment to maximize the intensity of mass transfer.

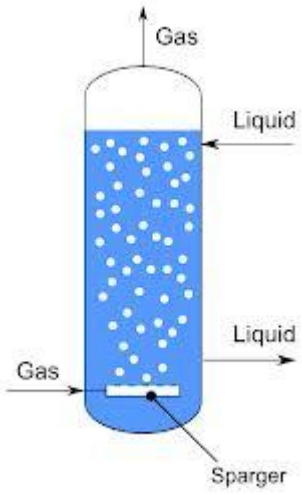

Fig1. Bubble column

A distinct feature of a bubble column is intense back-mixing of the liquid phase[5]. Despite its limitations due to back-mixing of gas phase or liquid phase, bubble columns in general offer many advantages over other multiphase reactors such as operation simplicity, minimal space requirements, the simplicity of their construction and maintenance, cost-effective technology, low energy consumption[1]. In Bubble Column flow regime can be homogeneous, heterogeneous or slug flow.

1.2) Important Performance Parameters of Bubble Column:

There are many parameters in bubble column which effects the efficiency of product. Some of them are gas distribution, flow regimes, fluid dynamics, bubble size, bubble rise, dispersion of the liquid, and the gas phase, gas holdup and specific interfacial area.[1]

a) Gas distribution: Usually, the gas is dispersed to create small bubbles and distribute them uniformly over the cross section of the equipment to maximize the intensity of mass transfer. The formation of fine bubbles is especially desirable in the homogeneous flow. Gas distribution is done by using spargers.

b) Flow regimes: The upward motion of bubbles gives rise to three distinct flow regimes. Homogenous flow is caused by narrow bubble size distribution and they are well spread uniformly among cross section of column. The uniform distribution of gas bubbles vanishes at higher gas rates, and a highly turbulent flow structure appears known as heterogenous flow in which bubbles agglomerate and travels with high velocities. Slug flow occurs at high gas flow rates usually in small diameter columns used for laboratory.

c) Bubble Size: Analysis of bubble size in bubble columns must distinguish between bubble-size distribution just after bubble formation at the sparger and size distribution further away from the distributor. Because of breakup and coalescence of the rising bubbles, the two distributions can differ significantly.

d) Bubble Rise Velocity: In the homogeneous flow regime, bubbles of almost uniform size and shape rise in the form of a swarm distributed uniformly over the column cross section, where in heterogenous regime larger bubbles are formed by agglomeration. These are having significantly higher velocity than the small bubbles. Thus the quantity of gas transported by larger bubbles linearly increases with gas velocity.

e) Gas Holdup: Gas holdup is a dimensionless key parameter for design purposes that characterizes transport phenomena of bubble columns[3]. Gas holdup is defined as the volume of the gas phase

divided by the total volume of the dispersion[20]. At high flow rates the gas holdup decreases in cocurrent systems because gas bubbles pass through the column more quickly. In contrast, the gas holdup rises in countercurrent systems[6]. The basic factors affecting gas holdup are: superficial gas velocity, liquid properties, column dimensions, operating temperature and pressure, gas sparger design, solid phase properties

1.3) ERT w.r.to Bubble Column:

Measurement of two-phase flow parameters are having much importance in many industrial processes such as physical, chemical and petroleum industrial processes. On-line measurement of two-phase flow parameters not only helps us analyze the effect of the flow pattern on phase fraction and flow rate measurement but also plays an important role in the safety of operation and the reliability of practical processes. ERT helps us to detect complex mixing conditions of two phase flow and to measure parameters involved inside a process vessel/tank. ERT uses conductive sensors on the wall of the process vessel to inject current and then sense voltage differences from which the conductivity of the electrolyte inside the process vessel can be measured using forward and inverse problems. It uses reconstruction algorithm to analyze the raw data obtained [6][4][9][10].

Many researchers attempted to characterize the bubble column and two-phase flow using the ERT/EIT in the past. Many of them measured the gas holdups, velocity profiles, rising velocities and bubble size distribution. M.wang et al (2000) concluded that higher viscosity fluid creates a higher hold up and used Linear back projection method (LBP) to reconstruct images. Yixin Ma et al (2001) concluded that combining the conventional ERT technique and the Liquid Level Detection method can greatly enhances the ERT system to monitor horizontal conductive gas/liquid pipe flow. A.D. Okonkwo et al (2012) studied the hydrodynamics of ionic liquids in a bubble column. Haibo Jin et al (2013) studied the characteristics of multi-stage bubble column which was having more advantages than conventional bubble column.

1.4) ERT Limitations:

ERT is yet to be implemented to the large scale industrial operations (large diameter vessels) the reason may be of noise issues in industrial areas as ERT is influential to noise generated by sensors.

The main drawback of ERT system is its low spatial resolution[2] and it is also sensitive to the electrodes location arrangements. The spatial resolution of the ERT is in the range of 3-10% of the equipment diameter. Limitations also includes that it cannot define the source of the conductivity change[14]. Using other technologies together with ERT may have the potential to further enhance its abilities and eliminate its limitations.[7]

1.5) Air-water Dispersive flow:

The gas-liquid dispersion is one of the most important characteristics and application of Bubble column. Due to the large-scale circulation flow both the liquid and gas phases are dispersed. The formation of large and small bubbles, coalescence, and breakup results in additional dispersion in the gas phase. Whereas the gas phase in a bubble column with a smaller diameter flows with virtually no back-mixing, large units behave more like stirred tanks[1]. The gas-phase dispersion depends mainly on gas velocity and column diameter than does that of the liquid phase. Even though the bubble column has simple geometry and operation, the flow behavior inside the bubble column is complex and is characterized by gas holdup profiles, radial, axial and tangential superficial gas velocities plots.

The liquid phase property has an impact on bubble formation and/or coalescing tendencies and hence is an important factor affecting gas holdup. An increase in liquid viscosity results in large bubbles and thus higher bubble rising velocities and lower gas holdup. Flow regime can be of homogeneous, heterogeneous and slug flow.

1.6) Significance of Bubble column Characteristics:

The gas holdup, Bubble size distribution, superficial gas/liquid velocity in the bubble column operation is important and they indicate bubble column performance. Radial gas holdup profiles were seen a sharper inclination at central region of column with an increase of gas velocity (Haibo Jin et al 2007), With increase in superficial gas velocity (SGV), solid and gas concentration (holdup) increases (Haibo Jin et al 2007). Gas holdup increases as ionic concentration increases and Velocity profile decreases with an increase in superficial gas velocity(A.D. Okonkwo et al 2012). Gas holdup increases with U_g (Superficial gas velocity) and radial distribution was high at centre of column for higher U_g (Haibo Jin et al 2013). Thus we can use ERT to know the effect of various parameters on gas holdup.

1.7) Scope of Work:

Electrical resistance tomography can be used to get tomographic images to characterize the gas-liquid flow in the bubble column. Image reconstruction algorithms are used to get the conductivity distributions inside the bubble column. Bubbles formation in the bubble column can be analyzed by using the ERT system. Effect of bubble size distribution and gas holdup can be predicted. Modified Sensitivity Back Projection algorithm, Linear back projection algorithm, Sensitivity coefficient back projection algorithm are used to construct the images from measured boundary voltages. The scope of this thesis is

- Obtain the gas-holdup profiles by using high speed electrical resistance tomography system.
- Validate the obtained gas-holdup profiles data with Image processing technique.
- Track the bubble size distribution by using the High speed camera.
- Compare the gas holdup profiles with different image reconstruction algorithms and different meshes for the ERT data analysis.
- Study the effect of design parameters and operating conditions of bubble column on gas holdup.

Chapter 2

Literature Review

In processes for converting natural gas to liquid fuels, bubble-column reactors are finding increasing application[3]. So the investigation of important hydrodynamic parameters has gained considerable attention during the past 30 years. Particularly, in recent years, most of researchers have focused on the following researches, such as gas holdup, flow regime, bubble parameters (bubble size, bubble velocity and so on) and flow velocity. Gas holdup is one of the most important operating parameters because it not only governs void fraction and also gas-phase residence time but is also crucial for mass transfer between liquid and gas. All studies examine gas holdup because it plays an important role in design and analysis of bubble columns. Gas holdup depends mainly on gas flow rate, but also to a great extent on the gas – liquid system involved. Gas holdup can be measured by Differential pressure, Electrical Tomography, Laser probe, Image processing, ultrasonics, X/γ-ray absorption methods, Positron emission Tomography(PET), etc

a) Pressure Differential method: The differential pressure method is widely used because of its simple apparatus and high accuracy[6]. A U-tube manometer or pressure transducers can be used to measure the pressure differences between any two points[7]. We can use below formula simply to calculate gas holdup[2][20]

$$\varepsilon = \frac{\rho_l - \frac{\rho g h}{H}}{\rho - \rho_g}$$

b) Image Processing: It is a method to convert an image into digital form and perform some operations on it. It is a type of signal dispensation in which input is image, like video frame or photograph and output may be image or characteristics or parameters associated with that image. It usually involves treating the image as a two-dimensional signal and applying standard signal-processing techniques to it[19]. It is among rapidly growing technologies today, with its applications in various aspects of a business. Image processing forms core research area within engineering and computer science disciplines too.

c) Tomography Methods: Currently, there are a number of tomographic techniques such as Positron emission tomography (PET), Magnetic resonance imaging (MRI), Ultrasonic systems, Optical and infrared tomography. Each of these techniques has its advantages,

disadvantages and limitations.[14] The choice of a particular technique is usually directed by many factors such as physical properties of the components of multiphase flow, the desired spatial and temporal resolution of imaging, cost of the equipment, its physical dimensions and human resources needs to operate it, and potential hazards to the personnel involved (e.g. radiation)[12].

Considering all these factors we concluded that Electrical tomography is one of the best available methods having the desired requirements. It is relatively fast up to 200 images per second and simple to operate, has a rugged construction and is sufficiently robust to cope with most of the industrial environments[14][16][7].

2.1) Electrical Resistance Tomography:

Electrical Resistance Tomography (ERT) is a measurement technique for obtaining information about internal structure or contents of a object or vessel non-intrusively[4]. Electrical Resistance Tomography (ERT) technique has greatly progressed since it was invented in the 1980s as a kind of Process Tomography technique[4][5][14]. ERT is a promising tool for the analysis of various unit operations, several process media, and for numerous purposes, with a lot of advantages, such as visualization, high speed, low cost, no radiation hazard, and non-intrusive, etc., it is a promising technique to monitor widely existing industrial conductive two/multi-phase flows, not only providing conductivity images, but also helps us to measure some flow parameters, such as void fraction, the flow regime identification, investigating a solid–liquid filtration process, packed columns, flotation columns, precipitation processes, hydrocyclones, bubble columns and measurements of the angular velocity It has been also used on process vessels such as mixers, pipes, reactors, and fluidized beds and on various aqueous conductive media such as water, saline, pseudo plastic fluids and dairy products. Application of ERT to other sectors such as food processing (applying to media such as juice, oil, and dressings) and environmental (applying to media such as waste water) remains to be discovered.[14][17]

2.1.1) Working Principle: An ERT system produces a cross-sectional image which helps us to know the distribution of conductivity of the contents of process vessels, from measurements taking at the boundary of the vessel. Working Principle of ERT is injecting a current between a pair of electrodes and measures the resultant voltage difference between remaining electrode pairs according to a predefined measurement strategy.[14]

2.2) ERT Hardware and Application:

ERT mainly consists of three parts known as Sensors (electrodes), Data Acquisition System (DAS) and a Host computer. Electrical resistance tomography (ERT) technique is mainly used in medical and mineral processing industries

Sensors: Sensor design is an important part of EIT as it plays a significant role in terms of the overall quality of data following image reconstruction. Electrical Resistance Tomography (ERT) sensors (Electrodes) can be used to obtain the conductivity data of two-phase flow at various positions, as well as information about the phase distribution and void fraction of the two-phase flow. The material for electrode construction depends largely on the process application. The material should be more conductive than the fluids being imaged in order to obtain reliable measurements[8][9][14]. Usually the electrode material is stainless steel, silver, gold, platinum, brass or silver palladium alloy.

Electrodes are arranged at equal intervals around the boundary of a circular vessel in a vertical series. Coaxial or triaxial cables are used to connect the electrodes, in order to reduce the noise. Traditionally, electrode configuration in ERT comprises numerous sensors (typically 16) arranged equidistantly around the boundary of a vessel or pipe.

Data Acquisition System: The Data Acquisition System (DAS) is responsible for obtaining the quantitative data describing the state of the conductivity distribution inside the vessel. The DAS is connected to the electrodes and the PC containing the image reconstruction algorithms. Depending on variability and sensitivity to conductivity changes, there are various data collection strategies to choose from, including adjacent, strategy, opposite strategy, diagonal strategy and conducting boundary strategy[12]. Adjacent strategy is the most common strategy in conventional ERT due to minimal hardware requirements and fast image reconstruction. The data must be collected quickly and accurately in order to track small changes of conductivity in real-time thus allowing the image reconstruction algorithm to provide an accurate measurement of the true conductivity distribution[14].

Host Computer: IT is a PC with control and data processing software installed which also records the measured values and is usually capable of on-line image reconstruction with the help of reconstruction algorithms pre-installed in it[14][12].

2.3) ERT Applications:

ERT is a measurement technique mainly used for characterization of two-phase flow of which atleast they should have one medium having electrical conductivity. So ERT can be used in many unit operations in chemical engineering such as bubble columns, pipes, separators, mixing vessels, reactors, digesters, and hydrocyclones. ERT was performed on horizontal pipes with various diameters between 35mm (Stephenson et al. 2007b) to 85mm (Xu et al. 2010a). In the cases of vertical pipes, diameters varying from 50mm (Hua et al. 2004) to 125mm (Tan and Dong 2006) have been investigated. ERT was also applied to the mixing and storage vessels varying from 15-40 cm in diameter (Miettinen et al. 2003;Simmons et al. 2009) to find out mixing characteristics. ERT was also applied to bubble columns by many researchers by placing the ERT above the gas distributor of acrylic-made bubble columns with inner diameters ranging from 5cm to 28cm (Fransolet et al. 2001; Wang et al. 2001; Fransolet et al. 2005;Toye et al. 2005; Jin et al. 2006; Jin et al. 2007, b; Vijayan et al. 2007; Jin et al. 2010).It was also applied to fluidized bed reactors (Razzak et al. 2007).

S.No.	Author (Year)	ERT system	Applications	Remarks
1	Haibo Jin et al (2000)	2-planes,16 electrodes, 2 frames/second	Measurement of gas holdup profiles in a gas liquid system	Transition regime cannot be obtained
2	D. Vlaev, M.Wanga, T. Dyakowski , R. Mann, B.D. Grieve(2000)	UMIST mark 1b-E DAS	Uneven filtrate flow, holes are partly blocked should be detectable by ERT	Reconstructed sections are not uniform although they are symmetrical
3	M.Wang et al(2001)	Single plane 16 electrode system,P2000 ERT system	Measurements of the concentration and velocity distribution in mixing of miscible liquids	Compared the tomographic data with the data obtained from conductivity probes

4	F. Dong et al(2005)	2-planes,16 electrodes, ERT system prototype	Measurement of disperse phase transient flow	ERT system is combined with the correlation method to gain the transient flow-rate of the disperse phase.
5	Chengzhi Tang et al (2006)	2-planes,16 electrodes, ITS Manchester, UK	Estimating Gas Holdup via Pressure Difference Measurements	More accurate gas holdup measurements can be made with pressure measurements
6	H. Jin, et al (2007)	2-planes, 16 electrodes	Analysis of bubble behaviors in bubble column	Results are in good agreement with conventional Pressure transmitter technique
7	Haibo jin et al (2007)	2-planes, 16 electrodes, ITS P 2000	ERT coupled with differential pressure measurement to determine phase hold ups in gas-liquid- solid outer loop bubble column	With increase in superficial gas velocity, solid and gas concentration (holdup) increases,
8	A.D. Okonkwo et al (2012)	2-planes, 16 electrodes, ITS P 2000	Characterization of a High Concentration Ionic Bubble Column	Effect of surface tension on ionic liquids.

9	Haibo Jin et al(2013)	2-planes, 16 electrodes, ITS P2000	Distribution Characteristics of holdups in a multi-stage bubble were studied.	With change in superficial gas velocity, significant change in gas holdup was observed
10	Mohadeseh Sharifi et al(2012)	2-planes,16 electrodes, ITS P2000	3-Dimensional qualitative analysis demonstrated the capability of ERT in detecting various undesired situations such as inhomogeneitydue to concentration, composition and temperature imbalances.	Possible with opaque solution like milk only
11	Haibo Jin et al(2010)	2-planes, 16 electrodes, ITS P2000	ERT application in three phase systems is limited to the measurement of phase hold-ups. Gas hold-ups and solid hold-ups increase with an increase in the superficial gas velocity increases.	Due to the limitation of Maxwell equation, the future work should be recommended to justify the accuracy of the combined technique for the three phase flow measurement.

Table 2.3.Literature Review of ERT w.r.to Bubble column

2.4) Reconstruction Algorithms:

The image reconstruction problem in ERT can be considered as an optimization problem.

The image reconstruction is one of the most important and difficult part of ERT technique. In Electrical tomography techniques one needs to reconstruct the internal conductivity (or resistivity) profile of an object from boundary measurements of voltages. Mathematically, ERT reconstruction problem can be characterized as a non-linear ill-posed inverse problem There have been significant advances made in recent years on practical aspects of the reconstruction problem as well as on

theoretical aspects[15]. Many reconstruction algorithms, such as Modified Newton-Raphson (MNR) algorithm, Back-Projection (BP) algorithm, Sensitivity Coefficient (SC) algorithm, have been reported (Jinhua et al, 2010). The choice of image reconstruction algorithm depends on accuracy of image and time required for reconstruction. In particular the most implemented techniques for reconstruction in ERT are filtered backprojection between equipotent lines (Barber, 1990); back projection using sensitivity coefficient (Kotre, 1989); perturbation method (Yorkey et al.,1987b); double-constraint method (Wexler et al., 1985); Newton–Raphson method (Abdullah 1993) and the SCG method (Wang, 2002). Recently Broyden-Fletcher- Goldfarb-Shanno (MBFGS) algorithm (Jinhua YU et al 2010) is studied by comparing with other algorithms.
Considering the total variation (TV) functional plays an important role in the regularization of inverse problems belonging to many disciplines, after its first introduction by Rudin et al (1992) in the image reconstruction area. The stability of the Tikhonov regularization method (TRM) algorithm is a bit sensitive to the setting of the starting value of conductivity. The optimal selection of the hyper parameter value ($\boldsymbol{\sigma}$) which is used in TRM provides balance between the accuracy and the stability of the solution (Kriz et al, 2009).ITS developed ERT system uses sensitivity back projection algorithm to get the conductivity images from the raw voltage measurements.

2.5) Literature review on Image Processing:

Bubble size measurement has been investigated for many years using a wide variety of techniques and approaches. Some methods for the size range include using conductivity probes (Lewis ***et al.,*** 1984; Barigou and Greaves,1996; Svendsen ***et al.,*** 1998), or fiber optics (Saberi ***et al.,*** 1995; Meernik and Yuen, 1988a,1988b) Electroresitivity, Anemometric Laser. Photographic techniques are among the most widely used methods in research on the bubble behavior. In particular, non-intrusive high-speed video observations coupled with digital image processing can provide valuable information regarding bubble size distribution (BSD).Recorded images (by HSV camera), were put into analysis either by the use of own software or commercial product (MATLAB). Digital processing of the flow images obtained using high-speed cameras can be used to estimate bubble size and velocity distribution and can allow individual bubble tracking. Unfortunately, the extraction of information about bubble size, shape and motion becomes more and more complicated with increasing gas hold-up as bubbles overlap each other.

S.No.	Author	Application	Remarks
1	Guadalupe Ramos Caicedo et al (2003)	Shape factor and aspect ratio were studied. CCD camera with resolution of 758/512 pixels has used	Gas flowrate must not be either too big or too small.
2	P.L.C. Lage et al(1998)	Bubble diameters and gas holdup were measured	Can't go beyond 5 cm/s of superficial velocity of gas
3	Teklay Weldeabzgi Asegehegn et al(2011)	Successfully studied bubble characteristics such as bubble aspect ratio, shape factor, bubble diameter and rise velocity.	
4	A. Zaruba et al(2005)	velocity distribution was studied using high speed cam	Experimental results shown higher variation.

Table 2.4 Literature Review of Image Processing w.r.to Bubble Column

.

Chapter 3

Experimental Procedure & Methodology

Several experiments were conducted to measure the gas holdup, conductivity profiles, the effect of sparger on the performance of bubble column with respect to the design parameters and operating conditions with ERT. In order to meet the objectives of this thesis the experimental readings are essential. Experiments were conducted in house-made bubble column of 4 inch inner diameter and made of acrylic glass to which ERT system is attached. Experiments were conducted by using tap water as liquid and compressed air as gas. The experiments were performed with different design parameters and operating conditions. The bubbly flow was captured by high speed video camera to know the effect of design and operating conditions on gas holdup. The Gas holdup profiles were extracted from the ERT system. The obtained results from ERT are validated with the image processing data.

3.1) Bubble Column Experimental setup:

In the present work, bubble column of 100mm inner diameter and 5mm thickness is used for ERT experiments. The dimensions of the bubble column are shown in figure-2 (a). Air is fed into the bubble column from the inlet set at bottom of the setup, below the sparger. Water is fed from the open top of the bubble column and we were having outlet for water at the bottom of the column. After filling the enough water in the bubble column, we stop the supply of water and starts sending the air to get the bubbly flow. Feed air flow rate is measured by rotameter connected to the pump which we uses to send the air. Four different concentrations of frother usually Methyl Iso-butyl Carbinol(MIBC) is added for every 5 different flowrates. Below is the picture of operating bubble column with ERT attached.

Fig 3.1 Experimental setup of ERT

The following table is for the 4-inch bubble column with water as the liquid and compressed air as the gas. The experiments are carried for 3 different spargers of having 1mm, 1.2mm and 1.4mm hole diameter.

S.No.	Gas Flowrate (lpm)	Sparger (mm)	MIBC(ml)	S.No.	Gas Flowrate (lpm)	Sparger (mm)	MIBC(ml)
1	2	1	0	**26**	2	1.2	4
2	3	1	0	**27**	3	1.2	4
3	4	1	0	**28**	4	1.2	4
4	5	1	0	**29**	5	1.2	4
5	6	1	0	**30**	6	1.2	4
6	2	1	1	**31**	2	1.4	0
7	3	1	1	**32**	3	1.4	0
8	4	1	1	**33**	4	1.4	0
9	5	1	1	**34**	5	1.4	0
10	6	1	1	**35**	6	1.4	0
11	2	1	4	**36**	2	1.4	1
12	3	1	4	**37**	3	1.4	1

13	4	1	4	**38**	4	1.4	1
14	5	1	4	**39**	5	1.4	1
15	6	1	4	**40**	6	1.4	1
16	2	1.2	0	**41**	2	1.4	4
17	3	1.2	0	**42**	3	1.4	4
18	4	1.2	0	**43**	4	1.4	4
19	5	1.2	0	**44**	5	1.4	4
20	6	1.2	0	**45**	6	1.4	4
21	2	1.2	1				
22	3	1.2	1				
23	4	1.2	1				
24	5	1.2	1				
25	6	1.2	1				

Table3.1 Design of experiments

3.2) Electrical Resistance Tomography (ERT) setup:

ERT technique is used in the present study to measure the gas holdup profiles and the effect of different design parameters and operating conditions of the bubble column on the gas holdup. This ERT technique gives the images based on different conductivity of fluids flowing inside the plane. It shows different colors for liquid phase and gas phase in the tomographic image.

The z8000 system is a high speed Electrical Resistance Tomography system that is suitable for applications such as pipe flow, flow in reactors and mixers. The instrument is designed based on a high-performance dual-plane EIT system with a data acquisition speed of 1000 dual frames per second. The ERT setup contains 3 parts known as sensors, DAS (data acquisition system) and the host computer. Sensors are connected to cylindrical section of bubble column as shown in figure, the part on the other side of the sensors are connected to the DAS. The host computer and DAS are connected through the cable. Equally spaced sixteen electrodes (sensors) were fitted on the periphery of the bubble column in each plane and there are two planes in the cylindrical section. The electrodes are of rectangular shape and are constructed of stainless steel material. All these electrodes are connected to the DAS via co-axial cables. The distance between the two planes is 14cm.

AC Current is passed from the data acquisition system to the electrodes. DAS is controlled by using the Its tool, software z8000 Electrical Impedance Tomography System, which is installed in the host computer. The measurement strategy is very important to know the conductivity distribution inside the bubble column through electrodes which are arranged around the boundary. Here adjacent electrode strategy is used to get the voltage and conductivity measurements using electrodes. Electric current is applied between one pair of electrodes and the resultant voltage differences among the remaining 13electrode pairs are measured by DAS. This procedure is then repeated for all other possible combinations according to the equation "n*(n-3)/2", where n is the number of electrodes in one plane of sensor. The adjacent strategy for voltage measurement and current injection is shown in the following figure-4.

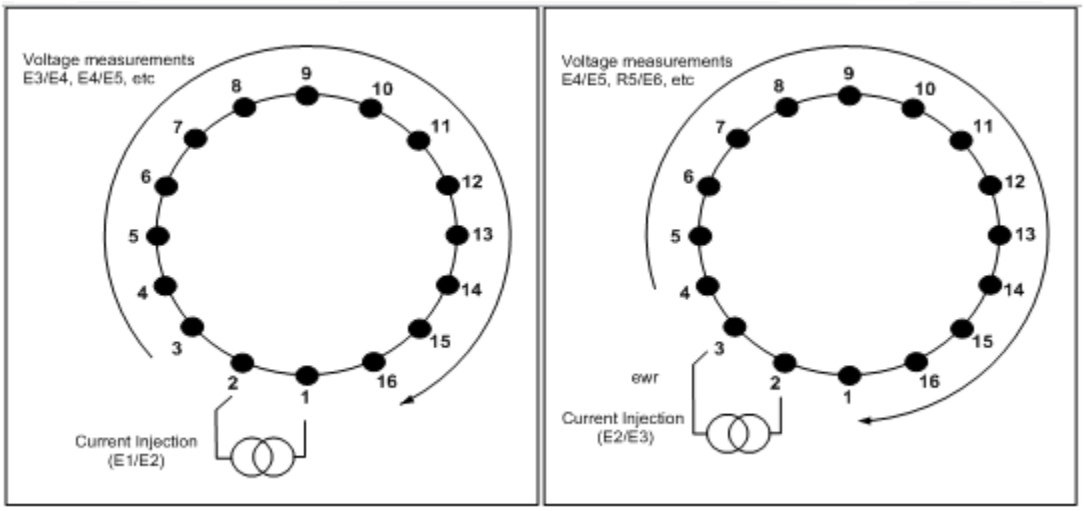

Fig 3.2 Current injection and voltage measurement sequence by adjacent strategy (Randall et al. 2005)

The host computer is connected to DAS system through the cable. This host computer is used to store and collect the data from the DAS system. After obtaining the voltage measurements from DAS system, the host computer processes data by using Image Reconstruction Algorithm. Sensitivity back projection algorithm and modified sensitivity back projection algorithm are used as the image reconstruction algorithm in the host computer to get the conductivity distribution inside the two planes.

3.3) Experimental procedure:

Experiments are conducted with the 4 inch bubble column and ERT system attached to it. The following picture-1 is the experimental setup of the ERT and bubble column. The process flow diagram of bubble column setup is also shown in picture-2. Air is pumped from the compressor to the duly filled bubble column with water. Tests were performed to determine the effect of air flow rate, sparger and frother addition on gas holdup in the bubble column. Prior to collecting the data by ERT, it is necessary to take a reference measurement since the system works on the principle of taking measurements and comparing these to known reference measurements. Initially bubble column is filled with the tap-water and reference is taken. Now we start sending the air into the bubble column, then bubbles start rising in the column and then we add 1 ml of MIBC to know the effect of frother. The diameter of the bubble column is 100mm and hole diameter of sparger is 1mm. For 2lpm air flow rate readings are taken this is repeated for next 2 times in order to get a consistent reading or to avoid human errors from the experiments. Data is collected for this 2lpm air flowrate by the ERT equipment and the procedure is repeated for 3, 4, 5 and 6 lpm. The same procedure is repeated for the 1.2mm and 1.4 mm sparger and also for the 2.5,3,4 ml of frother addition. The other design conditions of the bubble column were kept constant. The ERT system was employed to measure the conductivity of water and to get the required gas holdup profiles.

3.4) ERT Governing equations:

Electric field is generated from this strategy is determined from the Maxwell's equations

The relationship between the electric field and potential is

$$E = \nabla u$$

Ohm's law: current density (j) is directly proportional to applied electric field (E) and the proportional constant of the equation is called as conductivity ($\boldsymbol{\sigma}$)

$$j = \boldsymbol{\sigma} E$$

From the equation of continuity (Maxwell's equations)

$$\nabla . j = 0$$

Combining the above three equations gives

$$\nabla . (\sigma \nabla u) = 0 \qquad [1]$$

This governing equation gives is the electrical potential inside the bubble column.

In ERT an array of 16 electrodes are attached to wall of the bubble column. Ω and AC current with frequency of 1 to 100KHz is applied and resultant voltages are measured on remaining pair of electrodes. The above equation is solved by following boundary conditions.

1. The net current density through the surface of the electrode has to be equal to the total injected current.

$$\int \sigma \frac{\partial u}{\partial n} ds = I_l \qquad [2]$$

2. The surface measured voltages on each electrode consist of voltage on boundary surface underneath that electrode plus voltage drop across the electrode.

$$u + Z_l \sigma \frac{\partial u}{\partial n} = V_l \qquad [3]$$

3. When there is no current entering or leaving between the electrodes gap the current density equals to zero.

$$\sigma \frac{\partial u}{\partial n} = 0 \qquad [4]$$

Where,

V_l is surface measured voltage

I_l is injected current into l'th electrode, L is number of electrodes

Z_l is contact impedance between l'th electrode and object

The governing equation with above appropriate boundary conditions can be solved by numerical method. For complex geometry and boundary conditions finite element method is used for solving this equation.

3.5) Numerical solution of the forward problem:

Firstly we have to create a variational form or weak form of the original equation. Before getting the electric potential inside the domain from the variational form of the governing equation, is approximated with the linear combination of piecewise polynomial interpolation functions.

$$u(x) = \sum_{i}^{N} u_i \varphi_i(x)$$

Where $\varphi_i = \begin{cases} 1 & on\ the\ vertex\ i \\ 0 & otherwise \end{cases}$

The variational form of the equation is

$$\int \gamma \, \nabla.(\sigma \nabla u) dV = 0 \qquad [5]$$

Here γ is a test function which is approximated as

$$\gamma\,(x) = \sum_{i}^{N} \gamma_i \, \varphi_i(x)$$

Where $\varphi_i = \begin{cases} 1 & on\ the\ vertex\ i \\ 0 & otherwise \end{cases}$

Using vector derivative identity

$$\nabla.(\gamma\sigma\nabla u) = \gamma\nabla.(\sigma\nabla u) + \sigma\nabla u.\nabla\gamma$$

$$\gamma\nabla.(\sigma\nabla u) = \nabla.(\gamma\sigma\nabla u) - \sigma\nabla u.\nabla\gamma$$

By substituting the above equation in variational form of the equation [5]

$$\int \nabla.(\gamma\sigma\nabla u) dV - \int (\sigma\nabla u.\nabla\gamma) dV = 0 \qquad [6]$$

According to the Gauss Divergence theorem to the second term of the left hand side of above equation

$$\int \sigma\nabla u.\nabla\gamma dV = \int (\sigma\nabla u.n)\gamma dS = \int \sigma \frac{\partial u}{\partial n}\gamma dS \qquad [7]$$

The right hand side of the equation i.e. Surface integral is divided into two sections area under the electrode and area between the electrodes.

$$\int \sigma \frac{\partial u}{\partial n}\gamma dS = \int \sigma \frac{\partial u}{\partial n}\gamma dS + \sum_{l=1}^{L} \int \sigma \frac{\partial u}{\partial n}\gamma dS \qquad [8]$$

From the boundary condition equation [4] the first term of right hand side the of the equation becomes zero then the equation [8] becomes

$$\int \sigma\nabla u.\nabla\gamma dV = \sum_{l=1}^{L} \int \sigma \frac{\partial u}{\partial n}\gamma dS \qquad [9]$$

From the given boundary condition [3]

$$\sigma \frac{\partial u}{\partial n} = \frac{(V_l - u)}{Z_l}$$

Substituting the above expression in the equation [9]

$$\int (\sigma\nabla u.\nabla\gamma) dV = \sum_{l=1}^{L} \int \frac{(V_l - u)}{Z_l}\gamma dS \qquad [10]$$

Putting the test functions and electric potential approximations in the equation [10]

$$\sum_{i=1}^{N} \int \left(\sigma\nabla\varphi_i.\nabla\varphi_j\right) dV + \sum_{l=1}^{L} \int \frac{1}{Z_l}\varphi_i\varphi_j \, dSu_i - \sum_{l=1}^{L} \int \frac{1}{Z_l}\varphi_i \, dSVl = 0 \qquad [11]$$

From the boundary condition equation [2]

$$\int \frac{(V_l - u)}{Z_l} ds = I_l$$

$$\int \frac{V_l}{Z_l} ds - \sum_{l=1}^{L} \{ \int \frac{1}{Z_l} \varphi_i \, dS \} u_i = I_l$$

$$\frac{1}{Z_l}(e_l) V_l - \frac{1}{Z_l} \sum_{i=1}^{N} \{ \int \varphi_i \, dS \} u_i = I_l \qquad [12]$$

Where el is electrode area and the conductivity which is the above equation is approximated as a piecewise constant basis function on each control volume

$$\sigma = \sum_{i=1}^{k} \sigma_i \, \varphi \beta_i(x)$$

Where

$$\beta_i = \begin{Bmatrix} 1 & on\ element\ i \\ 0 & otherwise \end{Bmatrix}$$

By using this approximation for conductivity, conductivity can be taken outside of the integral for the above equation. For a set of current injection patterns the above equations can be written as a set of linear equations

$$\begin{bmatrix} A1 + A2 & A3 \\ A3^T & A4 \end{bmatrix} \begin{bmatrix} U \\ V_L \end{bmatrix} = \begin{bmatrix} 0 \\ I^K \end{bmatrix} \qquad [13]$$

Where

$$A1(i,j) = \sum_{i=1}^{N} \int \left(\sigma \nabla \varphi_i . \nabla \varphi_j \right) \mathrm{dV} = \sum_{k=1}^{k} \sigma_k \int \left(\nabla \varphi_i . \nabla \varphi_j \right) dV$$

$$A2(i,j) = \sum_{l=1}^{L} \frac{1}{Z_l} \int \varphi_i \varphi_j \, dS$$

$$A3(i,j) = \sum_{l=1}^{L} \int \frac{1}{Z_l} \varphi_i \, dS$$

$$A4(i,j) = \begin{cases} {}^{1}/_{Z_l}(e_l) & i = j \\ 0 & otherwise \end{cases}$$

I_k is the vector of injected currents

U vector of nodal voltages

V_L is vector of electrode voltages

The above equation [13] can be written in reduced form as

$$Au = b$$

Where 'A' is a global stiffness matrix, 'u' represents the Potentials at nodes and 'b' represents the boundary current. In this way calculating the potential values at nodes from given conductivity distribution and currents is known as the forward problem. Finding the conductivity distribution from the given boundary voltages and currents is called as inverse problem.

3.6) Inverse problem:

To determine the conductivity distribution σ from a finite number of boundary voltage measurements is known as inverse problem. ERT reconstruction problem is a non-linear ill-posed inverse problem.However a problem is said to be an ill posed problem when that particular problem has not having the at least three conditions (uniqueness, stability and existence). Special techniques must be used to recover a stable solution. Small changes in boundary measured voltages can cause large error in estimating the conductivity profiles. Minimization of squared norm of the difference between measured boundary voltages and calculated boundary voltages by using numerical methods is an important task of image reconstruction algorithm of ERT. In order to obtain the stable solution optimization process adopts particular techniques. This process is known as regularization.

The linear back projection algorithm back projects the voltage measurements to conductivity values within the pixels for all possible current injection and voltage measurement combinations using the sensitivity map calculated by the FEM. The calculation of A is obtained from the perturbation of power approach which is used to calculate the A1. The A1 is also known as Jacobian matrix. The calculation of this matrix is used in the image reconstruction technique. The simplest method to implement image reconstruction technique is linear back projection algorithm which is suggested by Kotre (1989). In Kotre's linear back-projection method, the normalized transpose of the Jacobian is applied to voltage difference data, yielding the conductivity update. Kotre approximated the inverse of the Jacobian matrix with its transpose.

$$d\sigma = J^T dv$$

Another technique for solving the EIT inverse problem is Tikhonov regularization, where a priori information is incorporated into the algorithm, the solution obtained via the prior information included. A linear Tikhonov regularized Gauss-Newton solution is shown in below

$$\delta\sigma = (J^T J + \alpha^2 L^T L)^{-1}(J^T J + \alpha^2 L^T L(\sigma_{ref} - \sigma_o)$$

4. Where L is a smoothing matrix containing the a priori information, α is the regularization (Tikhonov)

Parameter and σ_{ref} is conductivity distribution containing known geometric structures.

Total variation regularization is one technique to permit image regularization without imposing smoothing. To avoid the smoothing for medical and process imaging total variation technique is used.

Chapter 4

ERT data analysis

4.1) EIDORS

EIDORS (Electrical Impedance and Diffuse Optical tomography Reconstruction Software) is an open source software that provides free reconstruction algorithms for forward and inverse modelling for Electrical Impedance Tomography (EIT) and Diffusion based Optical Tomography in medical and industrial settings. The original EIDORS (initial version) software is based on the thesis of Vaukhonen (1997). EIDORS implemented a MATLAB package for two-dimensional mesh generation, solving the forward problem and reconstruction of the images. Several utility functions are provided to create common electrode and stimulation configurations. This format specifies the electrode positions, contact impedances, and stimulation and measurement patterns, and all supported algorithms are able to reconstruct images based on data provided. EIDORS software consists of four primary objects: data, image, forward model and inverse model. Each object is represented by a structure (Adler et al). All objects have the properties of a name and type. The name is arbitrary; it is displayed by the graphics functions, and could also be useful to distinguish objects in a user specified function. The type is used to identify the object type (i.e. data, image etc.). The most complex EIDORS object is the forward model, which is designed to represent the finite element model (FEM), electrode positions and properties, and stimulation patterns, as well as the pointers to functions to solve the forward problem on this model. So EIDORS online software package is adopted in this thesis in order to get the quantitative information and to do the mesh refining of the required planes. This EIDORS software package has number of MATLAB programs for various applications which is useful for refining of mesh and to reconstruct the image using various quantitative reconstruction algorithms other than the MSBP which is used in the ITS tool suite.

4.2) Raw data from ITS Tool suite

4.2.1) Calibration:

To prove that ERT is giving correct values of conductivity we have compared the readings of ERT with the readings of conductivity probe at different concentrations of salt solutions of 0%, 1 %, 3% and 5 %(wt/vol).We found the measurements of conductivity are almost same in both the ERT and Conductivity probe. The below figure gives us a clear idea about this.

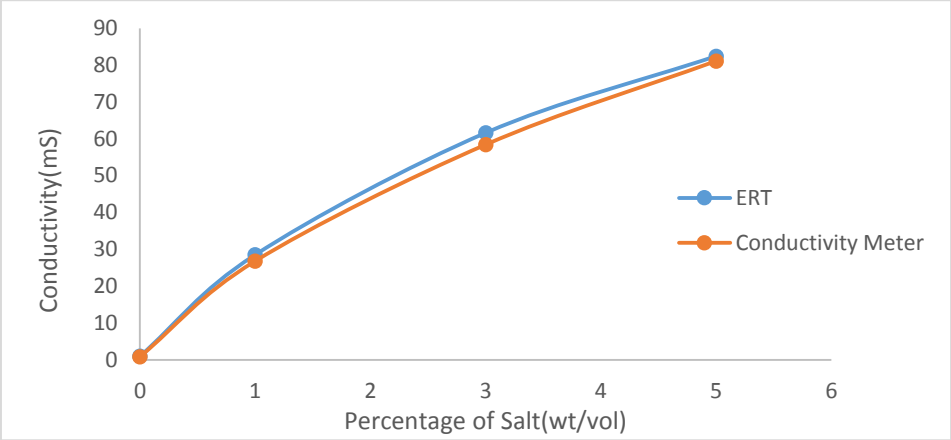

Fig 4.2.1 ERT Calibration

Using the adjacent measurement strategy of ERT to know the conductivity distribution inside the bubble column through electrodes which are arranged around the boundary. To know the conductivity value from the ERT, the data extracted from ITS toolsuite was used. An excel sheet was extracted from the time averaged tomogram which gives us the conductivity value of the mixture present in the bubble column and required excel sheets were extracted from the same tomogram to know the conductivity values at different positions along the cross section of bubble column where the cross section was represented by image reconstruction grid in the fig4.2.5

4.2.2) Voltage measurements:

Data was recorded at the 2000-2500 frames for every design and operating condition. Data was recorded using ITS z8000 system which helps us to record voltage measurements in the form of tomograms. Then after the data recording was finished voltage measurements were extracted from the tomogram which must be averaged to minimize errors in measurements, in the form of an excel sheet. 104 Voltage measurements were extracted from the tomogram in the form of an excel sheet. This excel sheet extracted from ITS toolsuite were used as input file in the EIDORS MATLAB package to calculate the conductivity distribution. The following figure was obtained from the

ERT system showing the reference voltage measurements, actual voltage measurements, and relative change between the reference and actual measurements. The vertical axis indicates voltage measurements (mv). The horizontal axis indicates the different electrodes pairs used for measurements from 1 to 13. P1 and P2 represents the two planes of the ERT system.

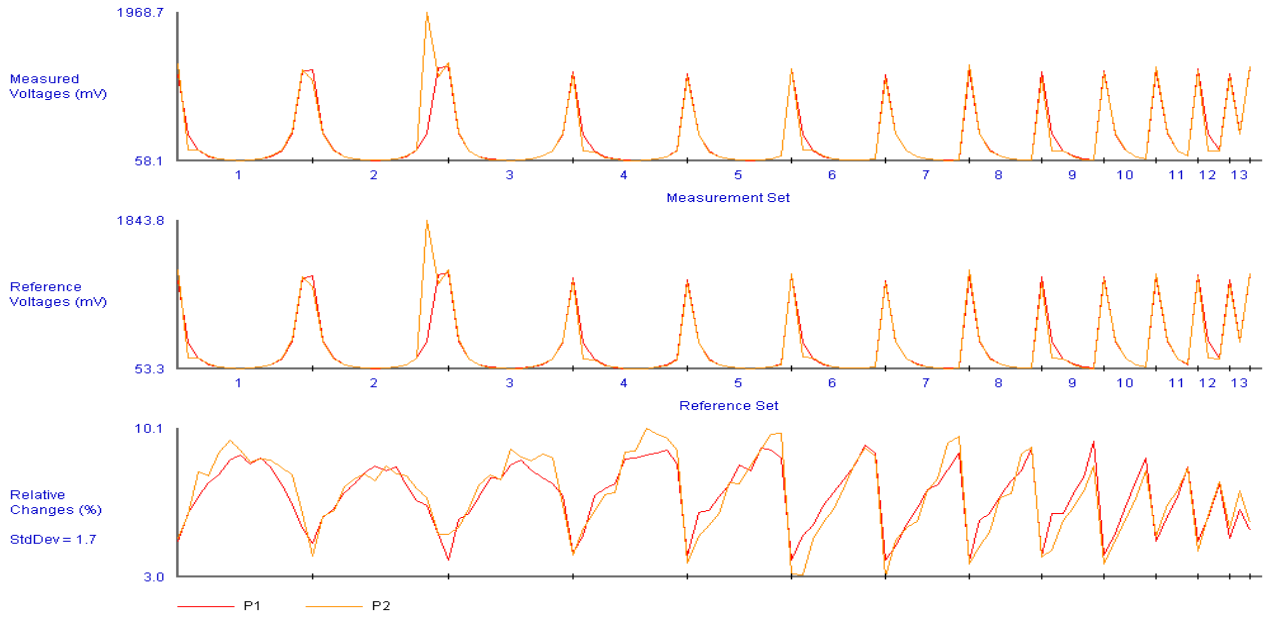

Fig 4.2.2 voltage measurements of Bubble column at two planes of cylindrical section by using ERT

4.2.3) Conductivity Tomogram

The mean conductivity tomogram was extracted to know the conductivity distribution across the plane-1 and plane-2 of ERT system along the cylindrical section of bubble column. Plane-1 and plane-2 are divided into 20x20 elements, where as some of the elements are out of the flow domain. So, only 316 elements were taken into consideration in such a way as shown in fig 4.2.5.The following figure represents the conductivity distribution across the bubble column across the two planes where electrodes are mounted internally to the wall of the cylindrical section of the bubble column. The figure shown was the image reconstructed by ERT system using Modified Sensitivity Back Projection (MSBP) algorithm which is the default algorithm used by ERT system to reconstruct the images.

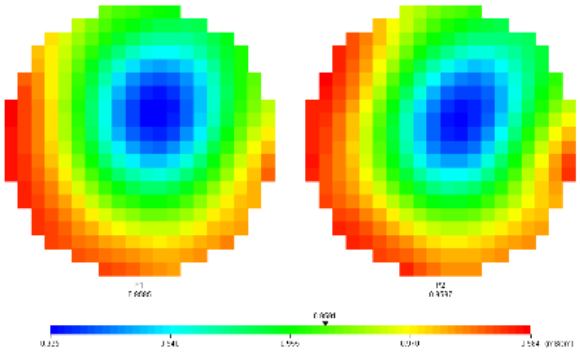

Figure 4.2.3 Mean Conductivity Tomogram

4.2.4) Concentration Tomogram

The concentration tomogram was extracted to know the concentration distribution across the plane-1 and plane-2 of the cylindrical section in bubble column. The following figure represents the concentration distribution inside the bubble column across the two planes where electrodes were mounted internally to the wall of the cylindrical section of the bubble column.

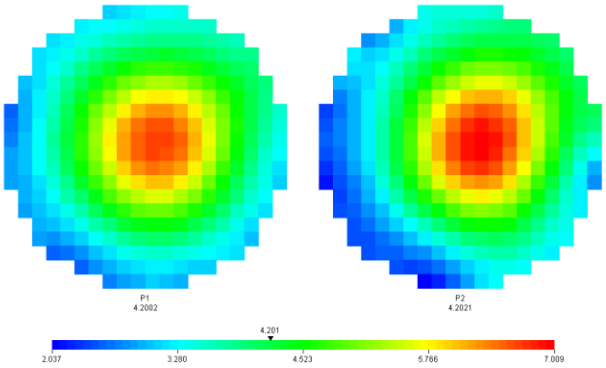

Figure 4.2.4 Mean Concentration tomogram

Volume fraction or concentration of air (non-conductive phase) is calculated by using Maxwell equation which is given as below [6]

$$\alpha = \frac{2(\sigma_1 - \sigma_{mc})}{\sigma_{mc} + 2\sigma_1}$$

Volume fraction or concentration of water (conductive phase) is calculated by using the following Maxwell equation [6]

$$\alpha = \frac{2(\sigma_1 - \sigma_{mc}) + \sigma_2 - (\frac{\sigma_{mc}\sigma_2}{\sigma_1})}{\sigma_{mc} - \frac{\sigma_{mc}\sigma_2}{\sigma_1} + 2(\sigma_1 - \sigma_2))}$$

Where α is volume fraction of dispersed phase

σ1 is the conductivity of continuous phase i.e. water.

σ2 is the conductivity of dispersed phase i.e. compressed air .

σmc is the reconstructed measured conductivity which is obtained from the conductivity tomogram.

4.2.5) Image reconstruction grid

Modified Sensitivity Back Projection algorithm is the reconstruction algorithm used in the ITS tool suite to reconstruct the images which results in tomograms. The mesh grid in this algorithm is 20X20 which results in a rectangular plane. As Circular plane is needed for bubble column some of those elements were removed as the sensors were in circular arrangement around the column. The following image is the mesh grid of the circular plane.

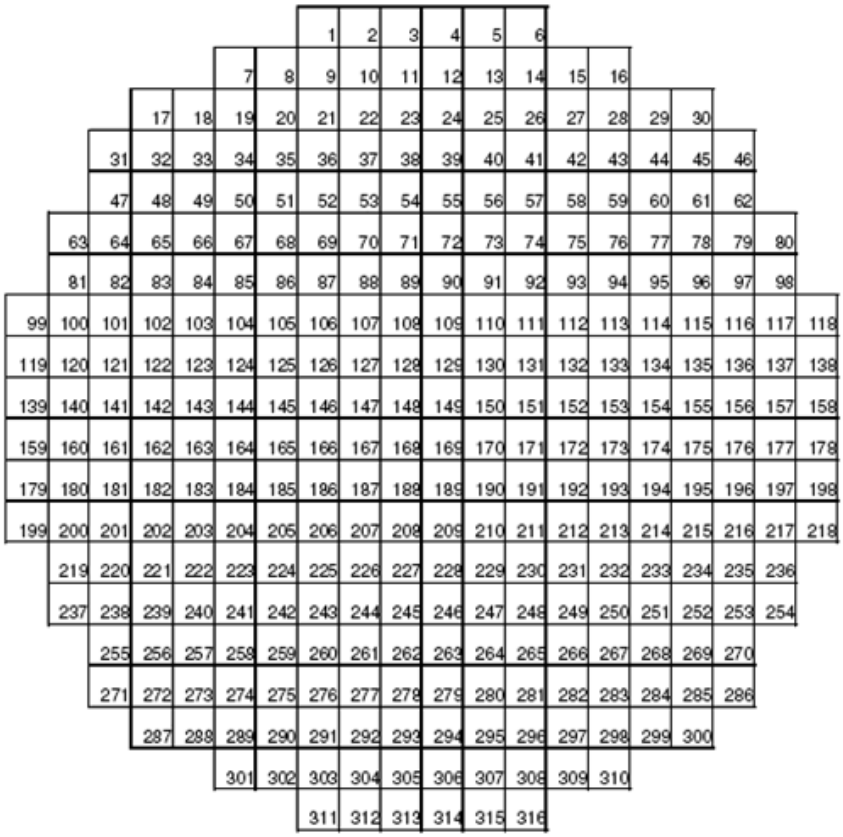

Fig 4.2.5 Image reconstruction grid

Conductivity tomograms obtained from the ERT systems for three different sparger diameters with different air flow rates is shown in the following figure. The results are following the theoretical trend qualitatively but not quantitatively.

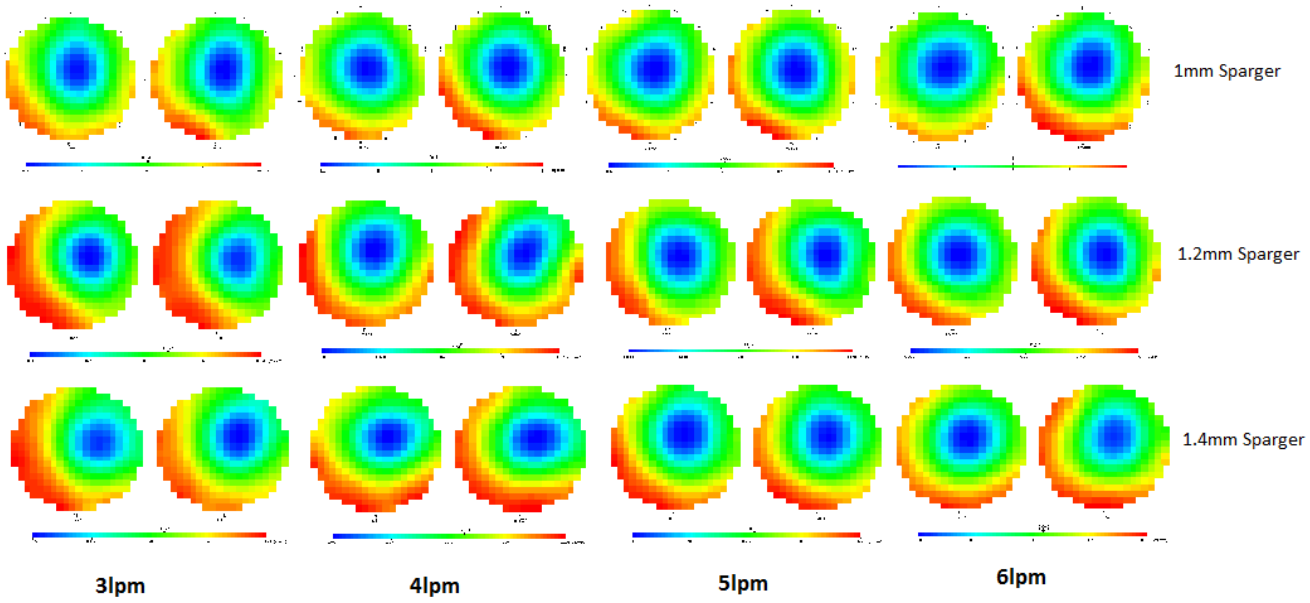

Fig.4.2.5(a) Conductivity tomograms for different spargers obtained from ITS Toolsuite

Data extracted from the ITS Tool suite is very diffusive in nature as MSBP reconstruction algorithm in ERT system uses coarse mesh. As the qualitative image reconstruction algorithm is used in ITS toolsuite, the information obtained from this gives only qualitative information. The reconstruction algorithms used in the ITS tool suite is limited. . So mesh refinement is not possible with the ITS toolsuite. So EIDORS online software package is adopted in this thesis in order to get the quantitative information and to do the mesh refining of the plane. This EIDORS software package has number of MATLAB programs for various applications which is useful for refining of mesh and all. The measured boundary voltages can be obtained from the domain conductivity which has uniform conductivity throughout the plane. These voltages are calculated from governing equation of the ERT system by using finite element method technique. Thus calculating nodal voltages of domain from the known current injection is known as forward problem. The EIDORS software has various mesh sizes for a domain. Using the FEM technique, the EIDORS software calculates the nodal voltages as well as boundary voltages. These boundary voltages are used to get the conductivity values at each node for non-homogeneous system. The EIDORS software has following mesh sizes for calculating the forward problem of the ERT system.

S.No	File name	No of elements
1	a2C	64
2	b2C	256
3	c2C	576
4	d2C	1024
5	e2C	1600
6	f2C	2304
7	g2C	3136
8	h2C	4096
9	i2C	5184
10	j2C	6400

Table 4.2.5 Number of elements for each mesh size

From the known surface voltage measurements calculating the conductivity values is known as inverse problem. For solving the inverse problem of ERT system image reconstruction algorithm is used. Number of image reconstruction algorithms is available in the EIDORS software. The following three image reconstruction algorithms are used to reconstruct the conductivity images

1. Tikhonov regularization
2. GN one step algorithm
3. Total variation algorithm

4.3) Sample data analysis:

Data analysis is done by using data set of five different air flowrates and sparger diameter of 1mm.The number of frames collected by using ERT system is 2500frames, voltage measurement was taken by making the average of the frames. These average voltages were given as an input file into MATLAB program which is generated by the functions and programmes from the EIDORS tool box from the MATLAB.

4.3.1) Effect of mesh on gas holdup:

The voltages generated from the averaging of the collected frames from the ERT system are used to get the conductivity distribution for different types of mesh. The mesh is used for calculation of conductivity and voltages by using the FEM technique. The following images are for different mesh sizes. From the following images we can observe that coarse mesh of b2C has high diffusive nature compared to other type of mesh sizes. From the f2C type mesh, diffusive nature of conductivity is very less.

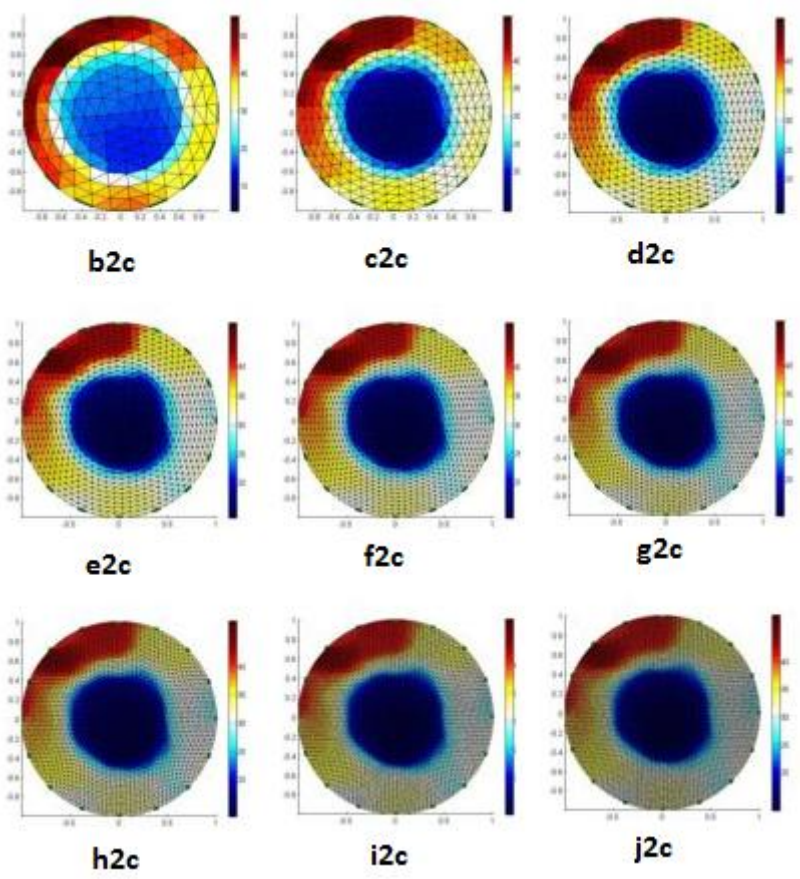

Fig 4.3.1 Effect of Mesh size on gas holdup

The conductivity plots across the radial position of the plane across the bubble column were plotted for various mesh sizes. It is found that the diffusive nature of conductivity is low for fine mesh when compared to the coarse mesh. So by increasing the mesh size, diffusive nature of the conductivity decreases. We have to select the optimum mesh size so that if you increase the mesh size the effect of diffusive nature is not observed. Optimum mesh size has to be selected to remove the effect of diffusive nature of conductivity.

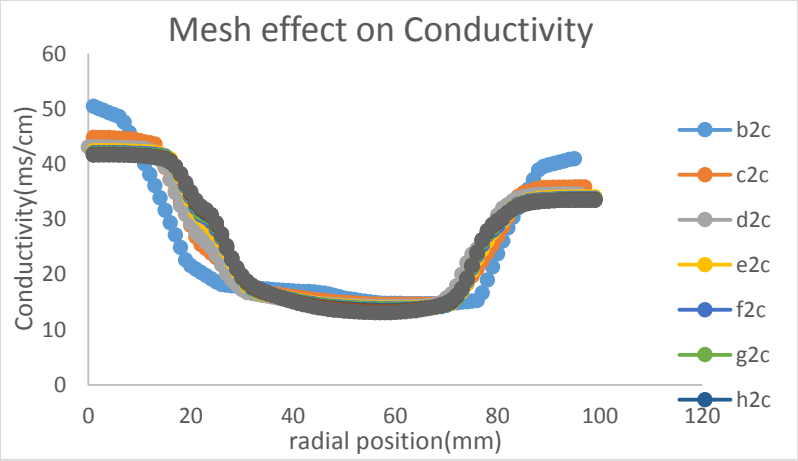

Fig 4.3.1(a) Radial conductivity profiles for different mesh sizes

4.3.2) Effect of Image Reconstruction Algorithm (IRA):

In this section we are discussing the effect of image reconstruction algorithm on the conductivity data of ERT. Firstly I am presenting the ERT tomogram for 5lpm which is reconstructed with the Modified Sensitivity Back Projection algorithm (MSBP) which is the default algorithm used by ITS tool suite to reconstruct the image. Then used this data in EIDORS to reconstruct the image by using different algorithms to know the effect of reconstruction algorithms.

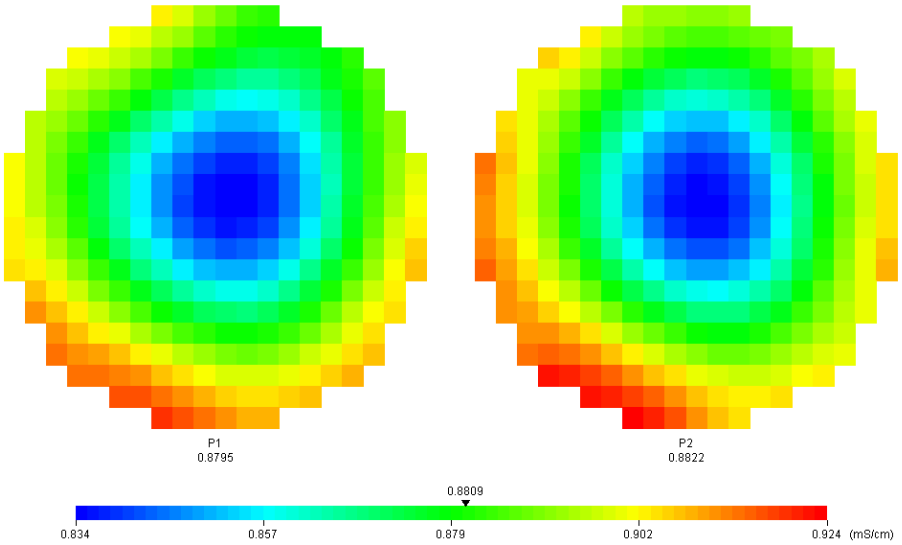

Fig 4.3.2 Tomogram obtained from ERT at 5lpm air flowrate

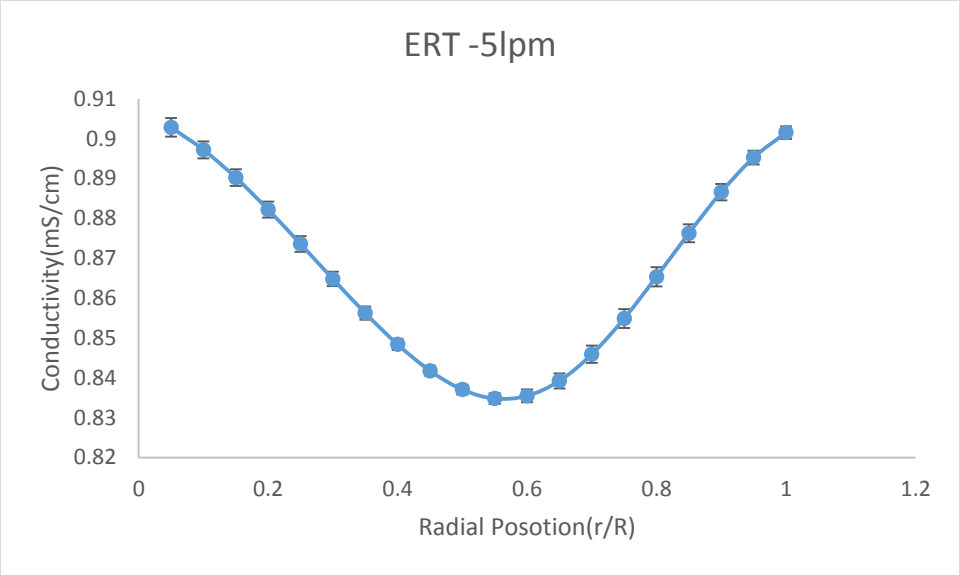

Fig 4.3.2(a) Conductivity Profiles obtained from ERT at 5lpm air flowrate

GN-one step, Tikhonov regularization and Total Variation image reconstruction algorithms are used to get the conductivity tomograms from the surface voltages. Compared the tomographic image obtained by these algorithms by ITS tool suit for 5lpm air flowrate and for 1mm sparger diameter of bubble column. The conductivity profiles were plotted for these three different image reconstruction algorithms.

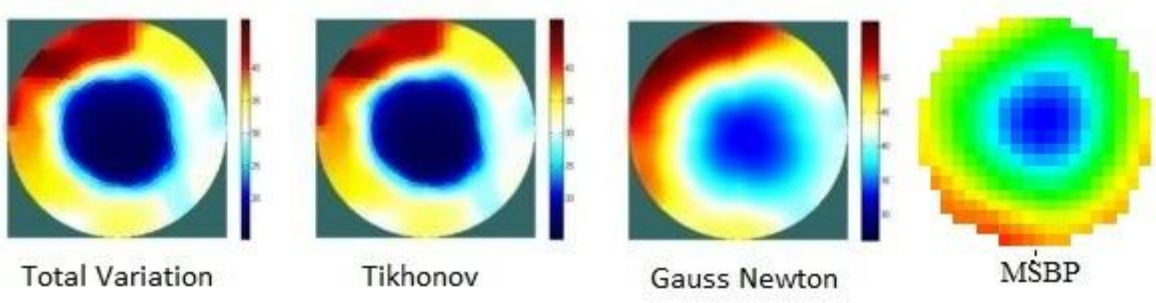

Fig 4.3.2(b) Tomograms obtained from EIDORS for different IRA

The conductivity distribution across the radial position of the bubble column was plotted for 2lpm air flowrate and 1mm sparger diameter is used. The conductivity profiles are compared with the three different image reconstruction algorithms. From the graph total variation and Tikhonov regularization algorithms are less diffusive in nature compared to the GN one step algorithm.

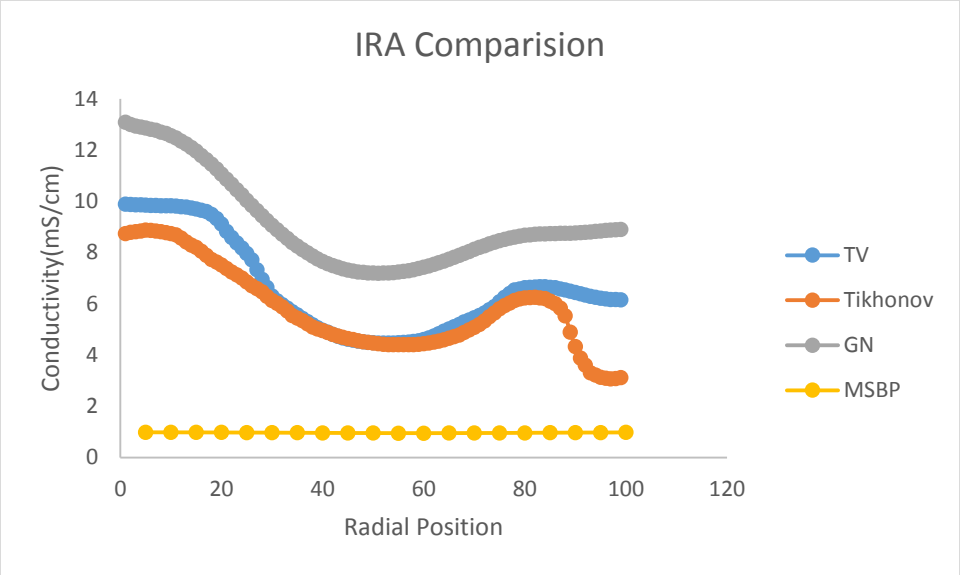

Fig 4.3.2(c) Radial Conductivity profiles for different IRA

Chapter 5

Results & Discussions:

In this chapter we focus on the results that were analyzed from the ERT and High speed video camera (HSVC) experiments. Variation of gas holdup with respect to the mesh size and image reconstruction algorithm were observed and the final conductivity tomograms were extracted using the EIDORS software. The effect of mesh and image reconstruction algorithm on gas holdup were discussed for one case that was used in chapter-4 of data analysis. Also the data is being analyzed for the bubble column operation for different design parameters and operating conditions in terms of the gas holdup.

5.1) Effect of mesh quality on gas holdup:

Here we are discussing the effect of mesh size on gas holdup for different flowrates and for different image reconstruction algorithms. The following results are acquired for 1mm sparger hole diameter. For every mesh size the tomograms are extracted for different operating conditions varying air flowrate from 2lpm to 6lpm. It is observed that the gas holdup varies with the mesh size. The effect of mesh size on conductivity distribution can be observed from the following results. Due to high numerical diffusivity of conductivity in case of coarse mesh, conductivity distribution is changed. The diffusivity of conductivity is low for fine mesh. The effect of mesh size for the f2C type which is having 2304 elements is negligible. So from these many types of mesh sizes the optimum mesh size can be selected as “f2C”, consist 2034 elements.

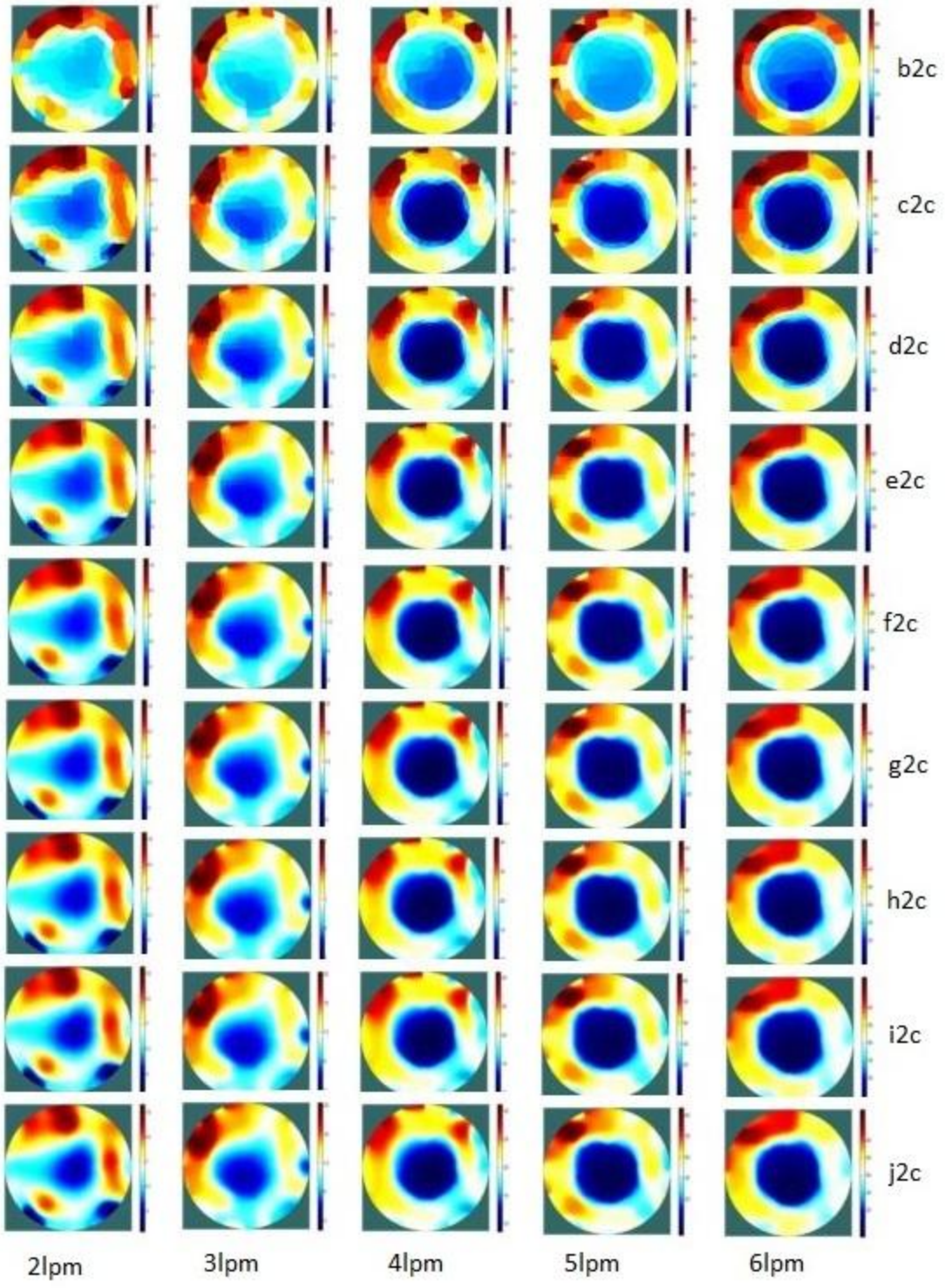

Fig 5.1 Effect of mesh for 1mm sparger w.r.t air feed flowrate

5.2) The effect of image reconstruction algorithms:

The effect of image reconstruction algorithms in extracting the conductivity tomograms has been shown in figure below with respect to different air flowrates. The tomograms are extracted for three different image reconstruction algorithms using EIDORS and Matlab. By using the three different algorithms namely Gauss Newton (GN), Tikhonov, Total Variation (TV) the conductivity tomograms are reconstructed for various design and operating conditions of the bubble column. The extracted tomograms shown here are for 1mm diameter of sparger with different operating conditions of air feed flowrate (2,3,4,5 and 6lpm respectively) are compared with three different image reconstruction algorithms. The tomograms extracted from the Total Variation regularization algorithm and Tikhonov regularization algorithm are having minimum diffusivity of conductivity profiles as compared to the Guass Newton one step algorithm.

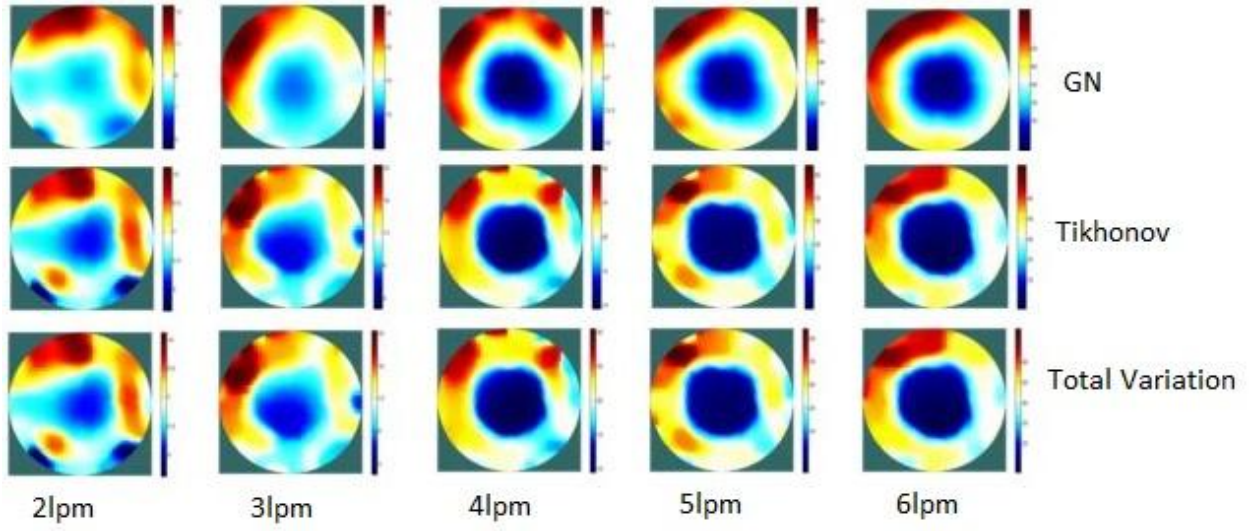

Fig 5.2 Effect of IRA for 1mm sparger w.r.t air feed flowrate

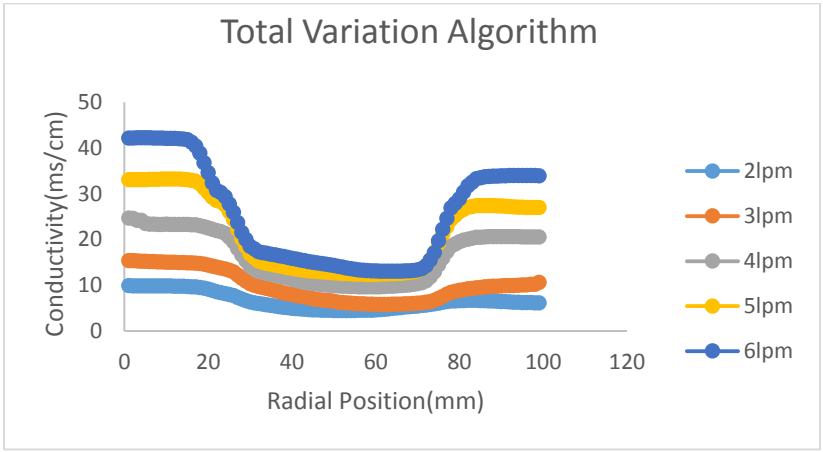

Fig 5.2.1 Radial Conductivity profiles obtained using TV algorithm

5.3) The effect of surfactant addition:

In this work surfactant was used for better determination of controlled bubble size and their characteristics. These studies are also used to know how the surfactant effects the gas holdup with respect to gas feed flowrate. Methyl Iso Butyl Carbinol (MIBC) was used as surfactant and experiments were conducted with three different concentrations of MIBC for three different spargers. Following are the ERT results obtained and one can observe that gas holdup value keeps on increasing with increase in gas feed flowrate. MIBC at low concentration (MIBC_LC) refers the 1ml addition of MIBC to the water present in the bubble column. MIBC at higher concentration (MIBC_HC) refers the 4ml addition of surfactant. MSBP reconstruction algorithm was used to determine the gas holdup values at different flowrates using the conductivity data obtained from ITS toolsuite. Gas holdup was calculated using the Maxwell equations mentioned in chapter 4.One can observe that the gas holdup value keeps on increasing with the addition of MIBC, this is because the rise velocity of bubbles decreases by increasing the surfactant concentration which results in decrease in surface tension [21].

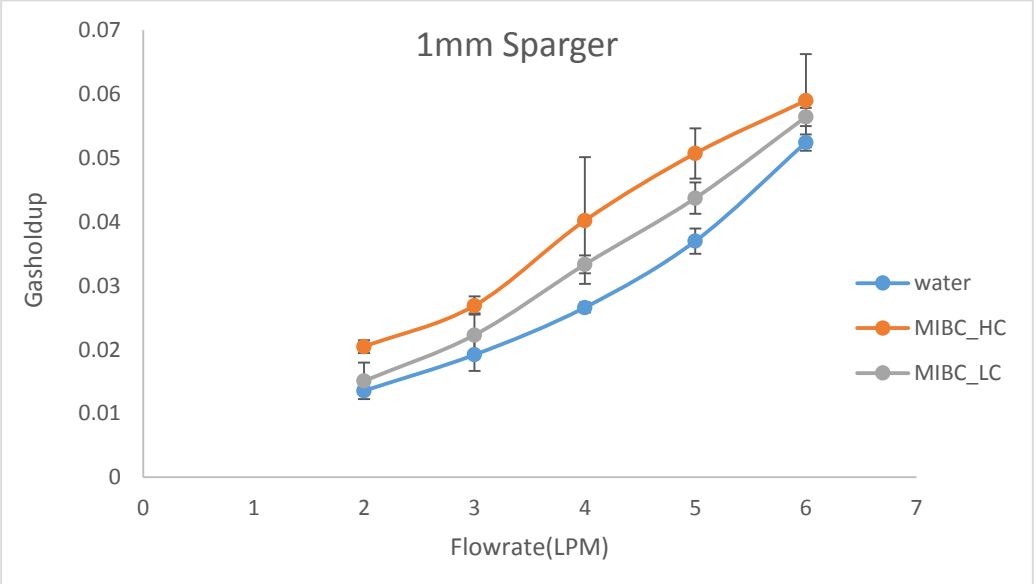

Fig 5.3.1 Effect of surfactant for 1mm sparger

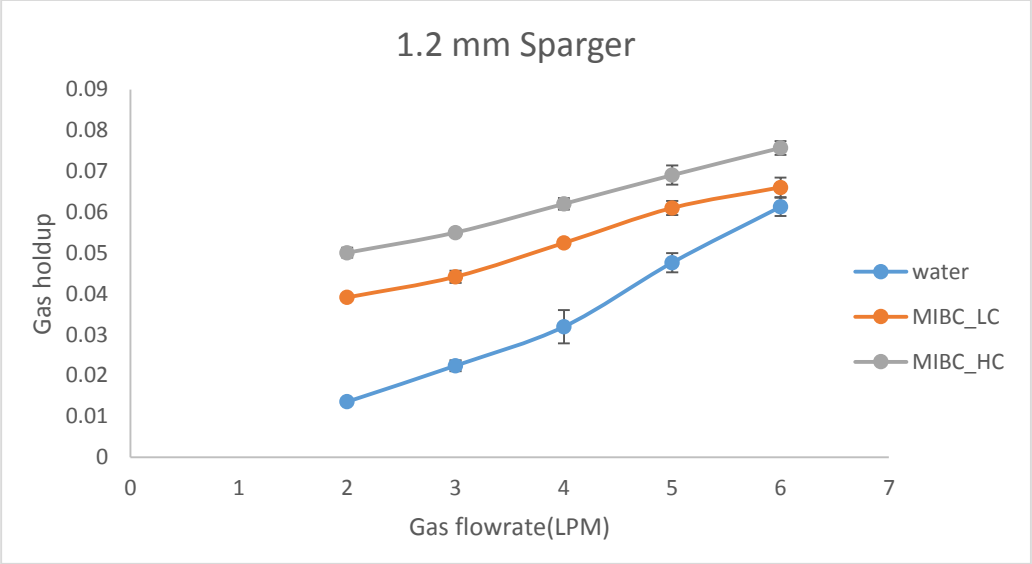

Fig 5.3.2 Effect of surfactant for 1.2mm sparger

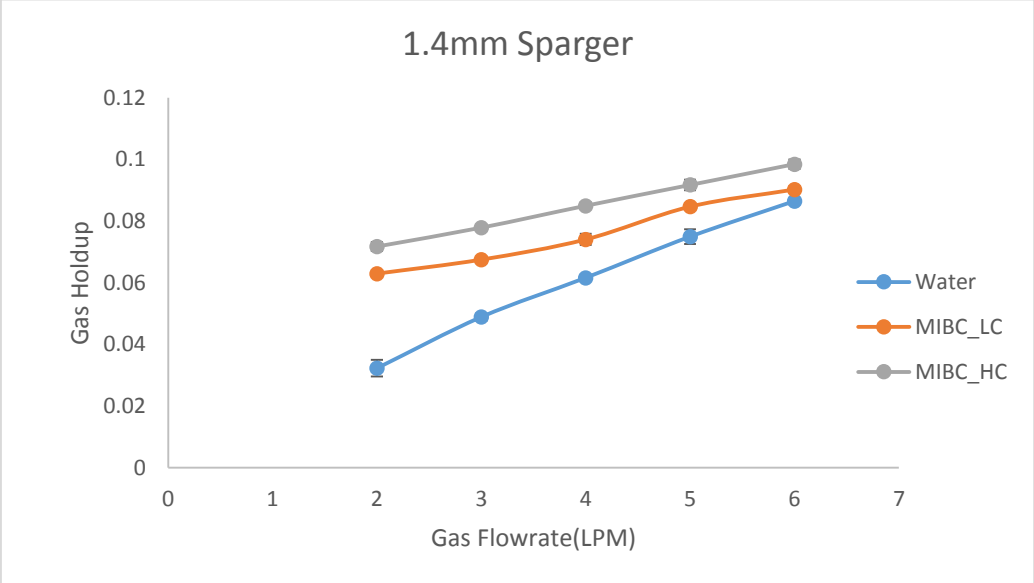

Fig 5.3.3 Effect of surfactant for 1.4mm sparger

From the above figures it was observed that after the 4lpm gas feed flowrate the gas holdup values are getting closer for all the different concentrations of surfactant.so below the 4lpm air flowrate surfactant has the influence on gas holdup, whereas higher gas velocity addition of surfactant increases the number of bubble. So addition of surfactant results in an increase in number of bubbles as surfactant helps to control the coalescence of bubbles resulting in smaller size of bubbles. Bubbles tend to become smaller with decreasing surface tension of water. Therefore, presence of surfactant increases the gas hold-up.

5.4) The effect of Sparger:

In this section effect of sparger is discussed with different concentrations of surfactant addition to water in the bubble column. Here higher concentration of surfactant refers the addition of 4ml of Methyl Iso Butyl Carbinol (MIBC) to water and lower concentration of surfactant refers the addition of 1ml of MIBC. Effect of sparger without addition of MIBC was also presnted. From the graph one can observe that with increase in sparger diameter results in increase of gas holdup.

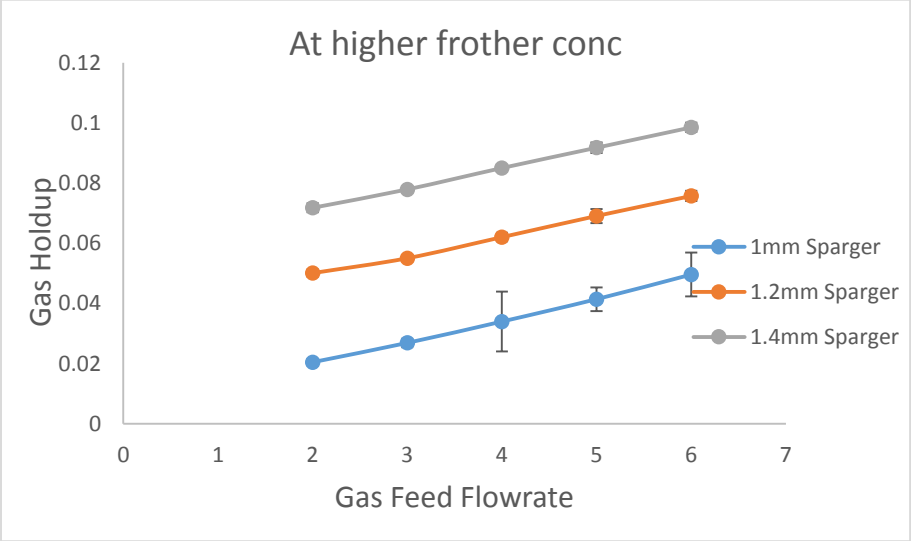

Fig 5.4.1 Effect of Sparger for higher concentration of surfactant

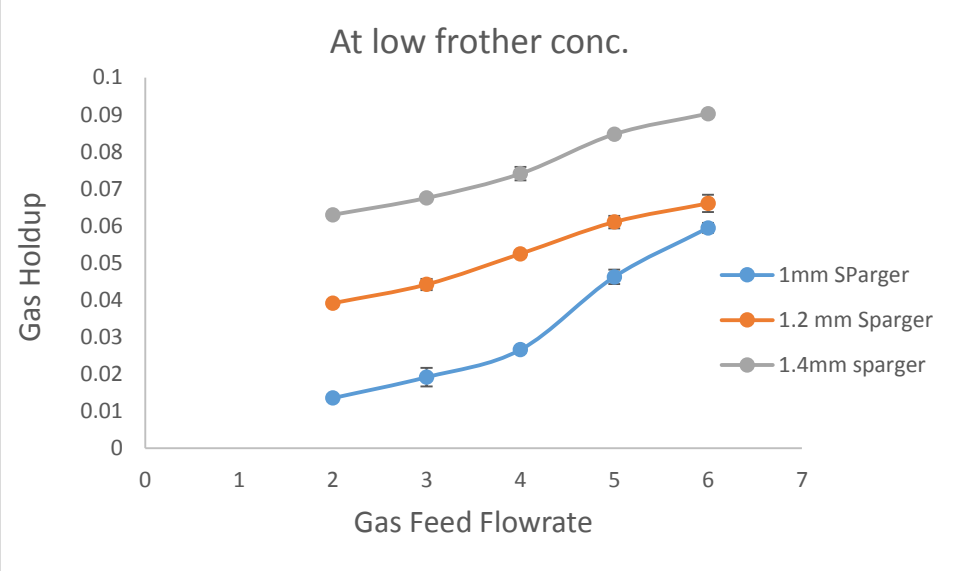

Fig 5.4.2 Effect of Sparger for lower concentration of surfactant

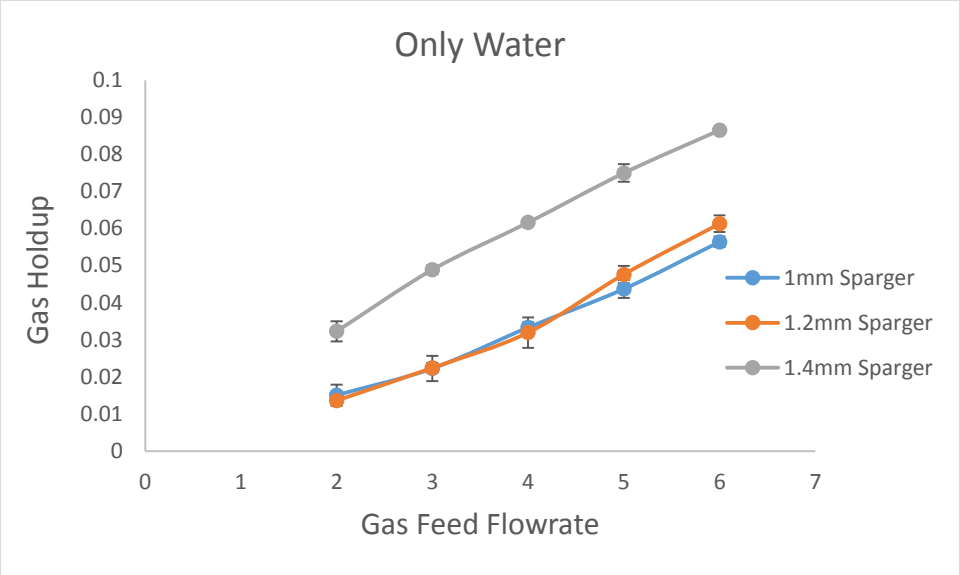

Fig 5.4.1 Effect of Sparger for zero concentration of surfactant

5.5) Results from High Speed Video Camera :

Here we've recorded the flow of the bubble column using Photron high speed video camera at the same experimental conditions which we had used for ERT experiments. The images captured were analyzed to know the bubble size distribution for different flowrates. High speed video camera captures the video from which we took snapshots and used them for data analysis. The images of the captured bubbles were analysed using a MATLAB program to perform a quantitative analysis of the images in order to obtain data on the sizes, shapes and orientations of the bubbles.

Fig5.5 Experimental setup of HSVC

5.5.1) Data analysis of High speed video camera:

We capture the video of the flow by using the high speed camera and then the video is converted into images and then the resultant image was used to get the required data. As mentioned before a MATLAB programme was used to find out the bubble size distribution by giving the recorded image as the input file to MATLAB program which gives us the information regarding size from the image based on the edge detection method. The process is described in the following steps:

1. Calibrating pixels: The length of the projected area was given in mm as the projected area was measured with scale during experimentation
2. Now six points were selected on the surface edges of bubbles. From analytic geometry, an ellipse can be defined by a specific set of five points: (x,y) to obtain parameters a,b,c,d and e in the ellipse equation $ax^2+bxy+cy^2+dx+ex+1=0$
3. Six points in the bubble edge were taken and a best fit of the 5 parameters was conducted to represent the ellipse.
4. The analysis yielded the long, a, short, b, axes and orientation angle,θ.

The volume-equivalent diameter approach was used to calculate the bubble diameter. It was assumed that the bubble depth was equal to the long axis, a, so the bubble volume equation might be expressed as follows i.e. an oblate spheroid. $V=(4\pi/3)a^2b$

Thus, the volume – equivalent diameter, d_e, is expressed as $d_e =2(a^2b)^{(1/3)}$

It was difficult in some parts of the image to identify the edge of the bubble because of their fast movement. Another disadvantage of the imaging analysis is that, with the bubbles close to the wall of the column, only the edge of the bubbles can be captured. So we compare this with ERT technique as the electrodes in this method were mounted on boundary of wall of column. Bubble size distribution curves were compared with the ERT data to know the compatibility of ERT experiments. Videos were recorded at the rate of 5400 frames per second and with resolution of 1024x1024. Following is the typical image captured using high speed video camera for 5lpm gas flowrate.

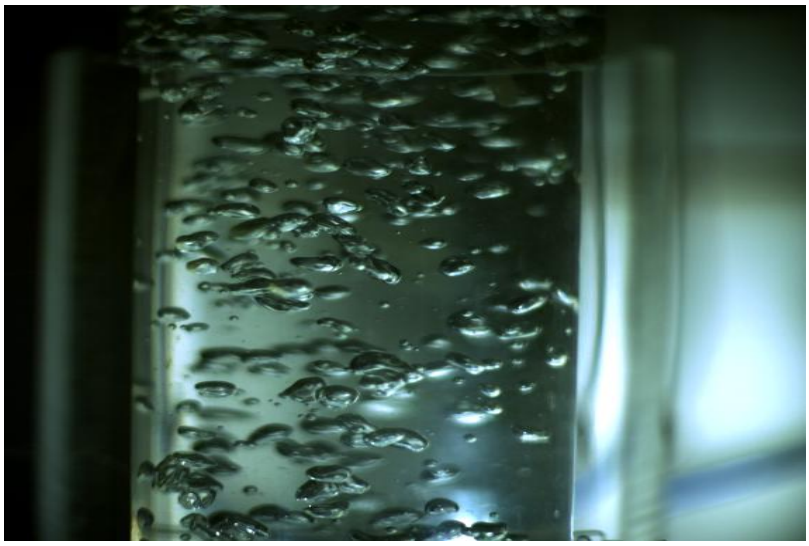

Fig 5.5.1 Image captured using HSVC at 5lpm air feed flowrate

Images were captured for different gas flowrates of 2,3,4,5 and 6 lpm and bubble size distribution was obtained for different flowrates and observed that bubbles are more in central region of bubble column. Following is the image in which bubbles were marked after giving the image as input file in the Matlab tool using Matlab imaging analysis codes.

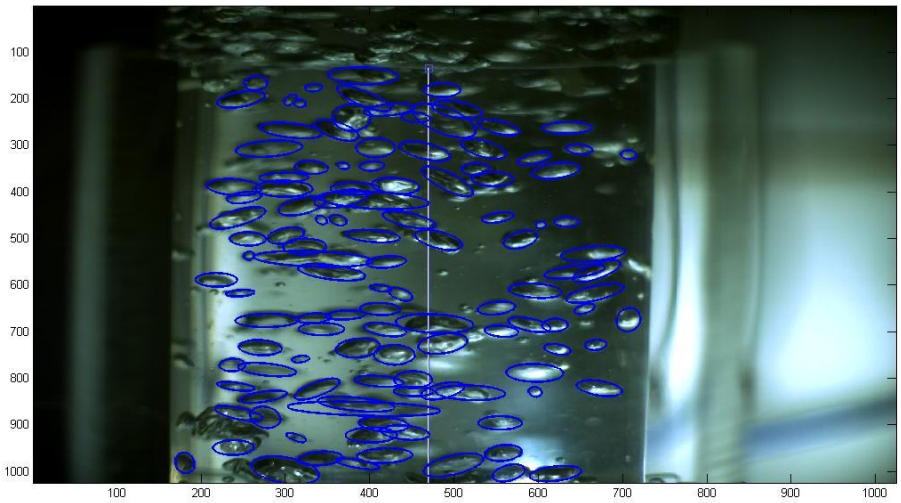

Fig 5.5.2 Marking of bubbles using MATLAB programme at 5lpm air feed flowrate

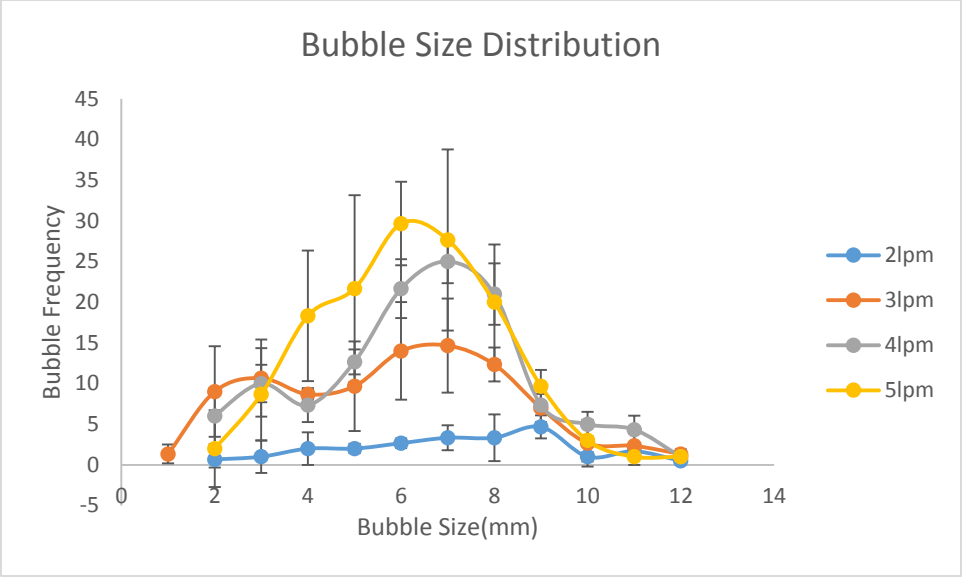

Fig 5.5.3 Bubble size distribution obtained from HSVC experiments

From the plot above we have observed that bubble frequency at the central region of bubble column got increased with increase in gas flow rate. The same graph above was represented as bar diagrams at each gas feed flowrate below.

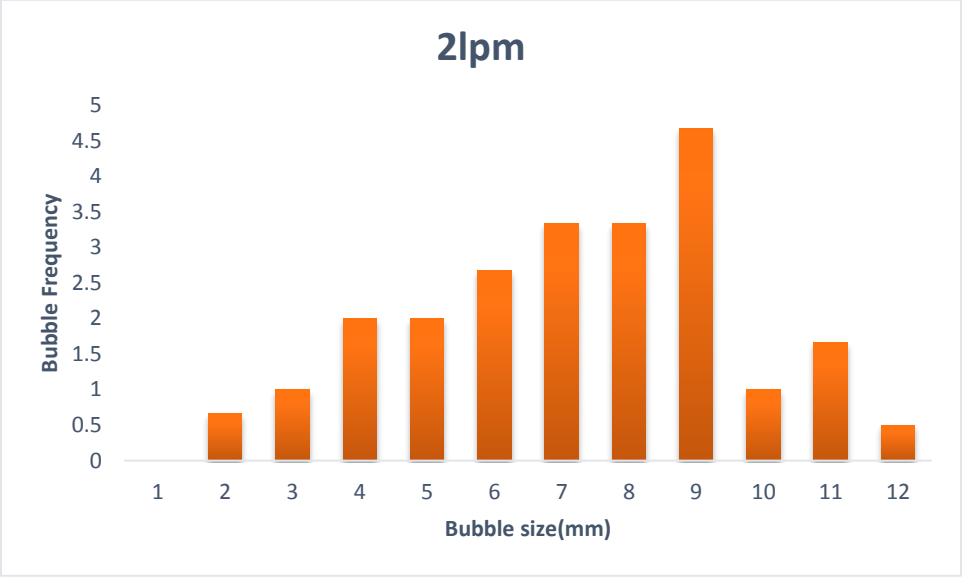

Fig 5.5.4 Bubble size distribution at 2lpm gas feed flowrate obtained from HSVC experiments

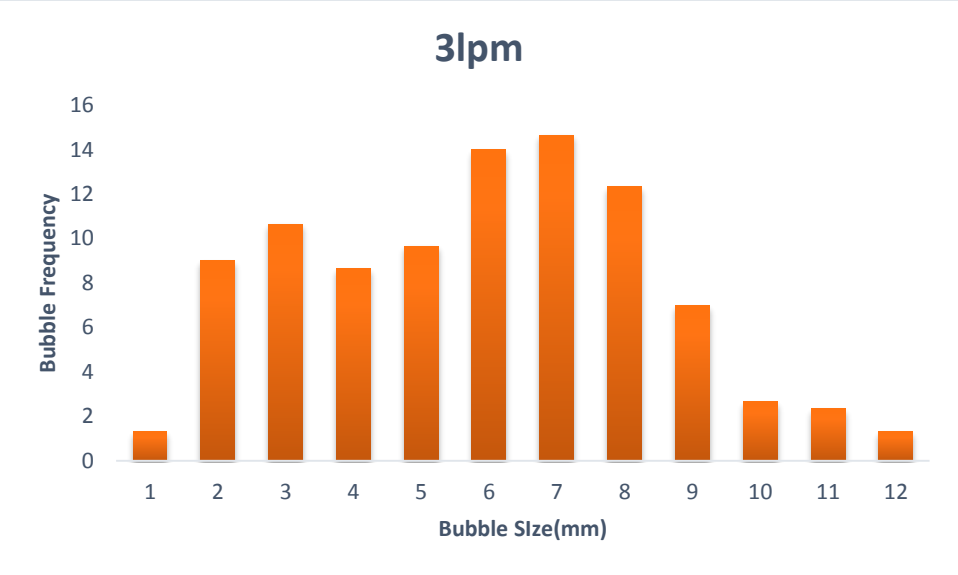

Fig 5.5.5 Bubble size distribution at 3lpm gas feed flowrate obtained from HSVC experiments

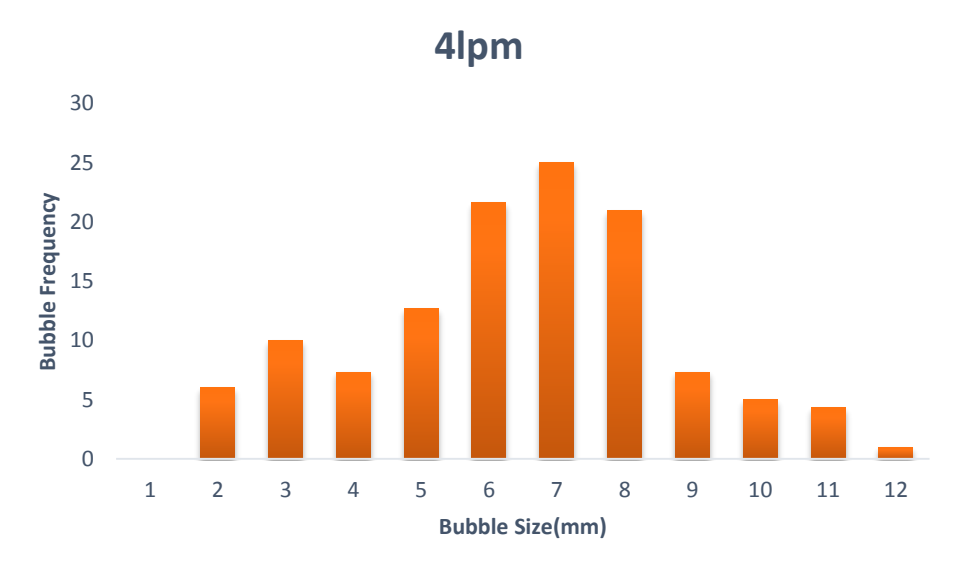

Fig 5.5.6 Bubble size distribution at 4lpm gas feed flowrate obtained from HSVC experiments

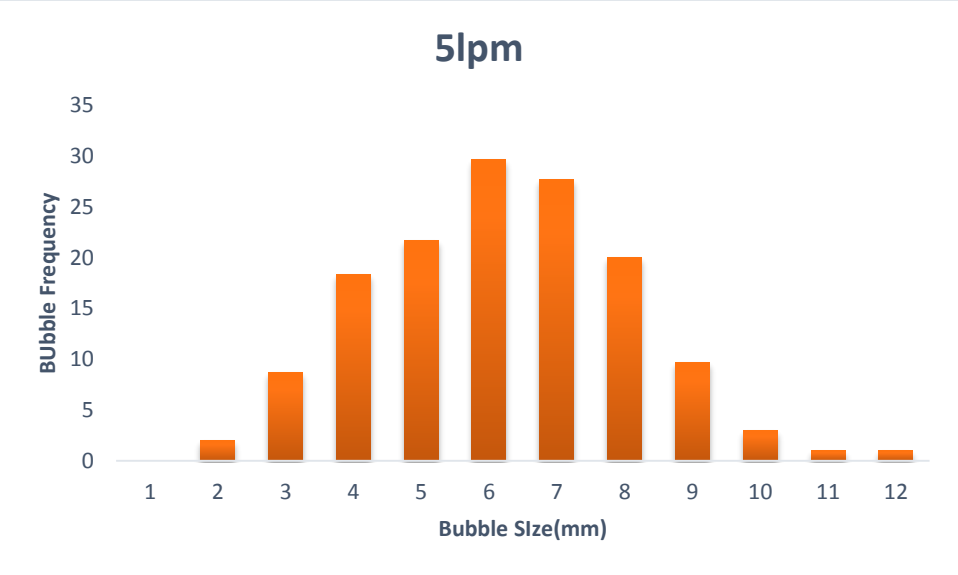

Fig 5.5.7 Bubble size distribution at 5lpm gas feed flowrate obtained from HSVC experiments

As air feed flowrate increases, large bubbles disappear and smaller bubbles prevail. However, the large bubbles are only observed at low gas feed flowrate. The size estimated from image processing supported this observation. Above bar diagrams gives us a clear idea about it.

Chapter 6

Validation of ERT data

The obtained conductivity profiles and gas holdup profiles from ERT are compared with the results derived from the high speed video camera. Results for 1mm sparger with no addition of MIBC and for different gas flowrates are compared in fig 6.1. It has been observed that bubble size distribution is more at central region of bubble column and gas holdup value increases with the increase of gas feed flowrate. Almost the same trend was observed with the ERT data obtained and percentage of error was estimated as 36.146 %.Also compared the ERT results of 1.2mm sparger and 1.4mm sparger with the results of high speed video camera for the same size of spargers and error percentage was estimated as 47.29% and 68.79% for respective spargers.

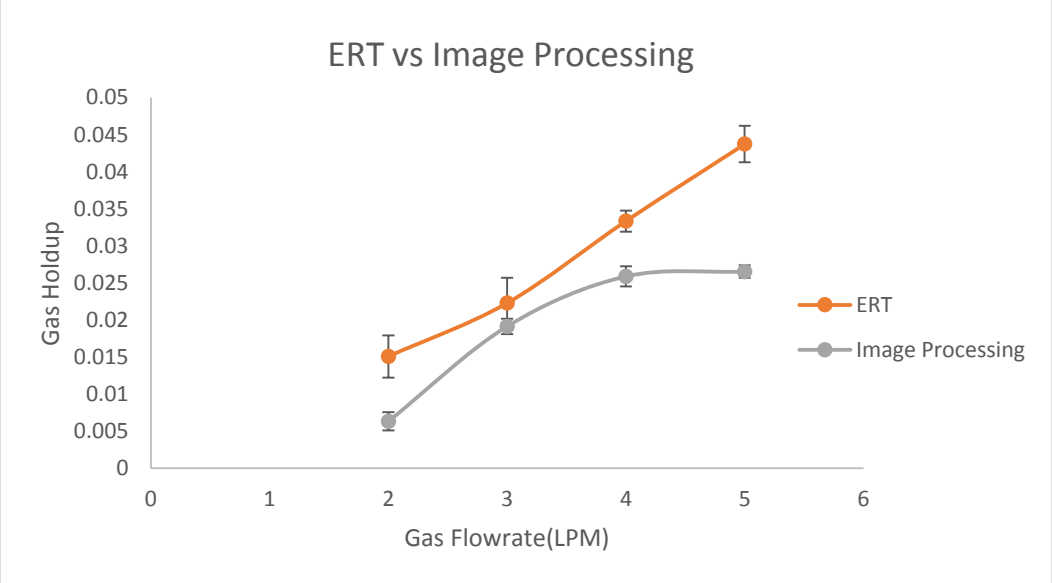

Fig 6.1 Validation of ERT Gas holdup profiles with Image Processing for 1mm Sparger

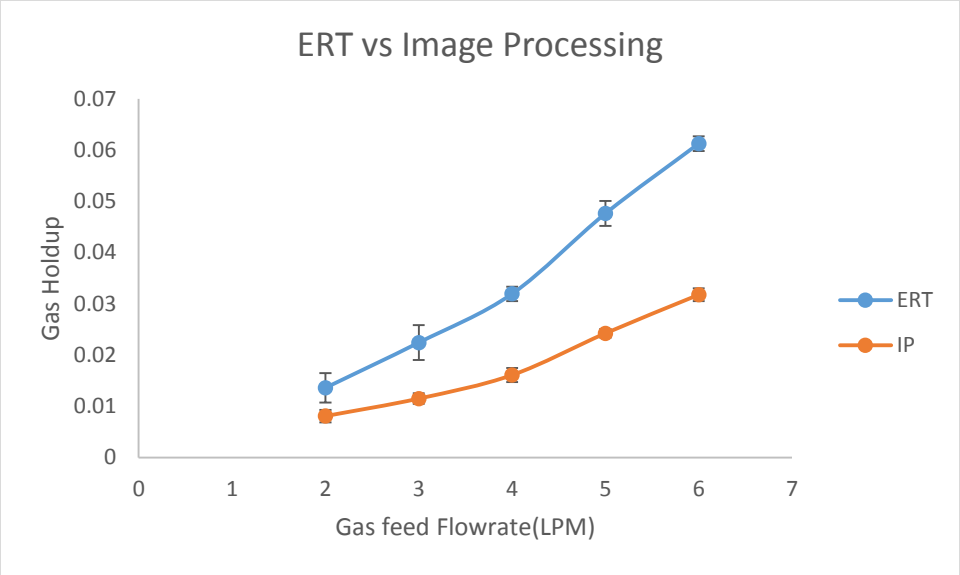

Fig 6.2 Validation of ERT Gas holdup profiles with Image Processing for 1.2 mm sparger

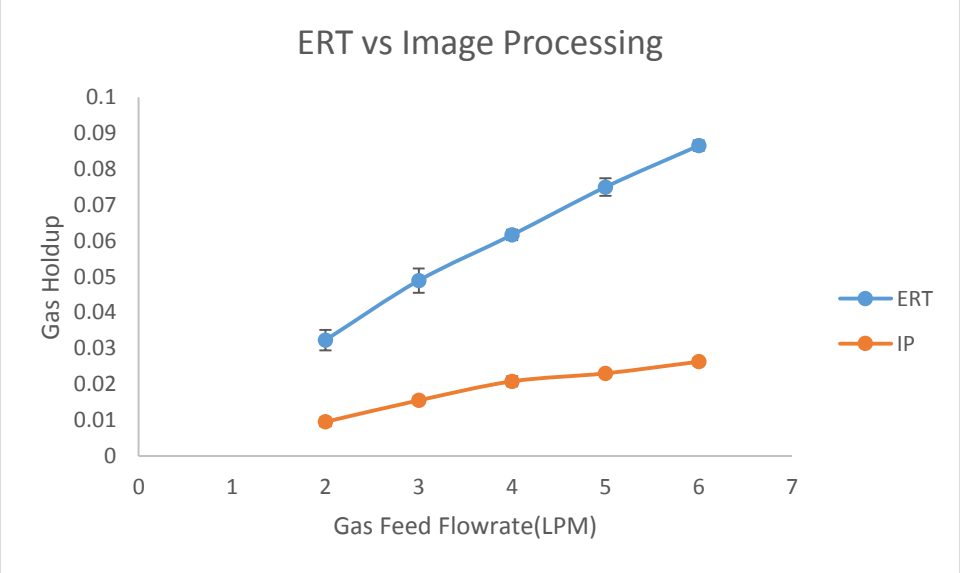

Fig 6.3 Validation of ERT Gas holdup profiles with Image Processing for 1.4 mm sparger

Chapter 7

Conclusions and Future Work

In this thesis the gas holdup was measured using the ERT system, EIDORS software and High speed video camera technique. The qualitative gas holdup profiles were obtained by ERT system. The gas holdup profiles using three different image reconstruction algorithms were extracted using EIDORS software. Numerical solution to the forward problem of the ERT system was presented. MATLAB programs were written by us to extract the conductivity profiles of fluid flowing inside the bubble column along the various radial positions at ERT planes by giving the boundary voltage data as input which was obtained from the DAS system of ERT. The obtained radial conductivity profiles from the EIDORS software were used to get the gas holdup profiles. The measured gas holdup profiles by Image Processing and gas holdup profiles obtained by the ERT system shows qualitative agreement with theoretical trends. The bubble size distribution was obtained using high speed video camera for various operating and design conditions of bubble column. The gas holdup with respect to different flowrates and for various sparger diameters were plotted. With increase in the feed gas flow rate the gas holdup keeps on increasing, was investigated through the ERT and EIDORS.

Future Work:

- Measuring the bubble size distribution by developing new MATLAB code which should auto detect the bubbles in the image given.
- New algorithms can be implemented to measure accurate conductivity distributions inside the bubble column using ERT system.
- Development of CFD model and validating with respect to ERT data.

References :

1) Peter Zehner, BASF Aktiengesellschaft, Ludwigshafen, Federal Republic of Germany Bubble Column Technology, 2005 Wiley-VCH Verlag GmbH & Co. KGaA, Weinheim
2) H. Jin a, M. Wang, R.A. Williams, Analysis of bubble behaviors in bubble columns using Electrical Resistance Tomography, Chemical Engineering Journal 130 (2007) 179–185
3) Rajamani Krishna, Jeroen W. A. de Swart, Jurg Ellenberger, Gilbert B. Martina, and Cristina Maretto, Gas Holdup in Slurry Bubble Columns: Effect of Column Diameter and Slurry Concentrations, AIChe Journal, February 1997, Vol. 43, No. 2
4) Jin Haibo, Lian Yicheng, Yang Suohe, Guangxiang He, Zhiwu Guo, The Parameters Measurement of Air-Water Two Phase Flow Using Electrical Resistance Tomography (ERT) Technique in a Bubble Column, Flow Measurement and Instrumentation, November 2012
5) Haibo Jin, Yicheng Lian, Yujian Qin, Suohe Yang, Guangxiang He, Distribution characteristics of holdups in a multi-stage bubble column using electrical resistance tomography, Particuology 11 (2013) 225– 231
6) Haibo Jin, Suohe Yang, Mi Wang, R.A. Williams, Measurement of gas holdup profiles in a gas liquid cocurrent bubble column using electrical resistance tomography, Flow Measurement and Instrumentation 18 (2007) 191–196
7) Haibo jin, yuhuan han, suohe yang, guangxing, He, Electrical resistance tomography coupled with differential pressure measurement to determine phase hold-ups in gas-liquid-solid outer loop bubble column, Flow Measurement and Instrumentation 21 (2010) 228-232.
8) Yixin Ma, Zhichu Zheng, Ling-an Xu, Xiaoping Liu, Yingxiang Wu, Application of ERT System to Monitor Gas-Liquid Two Phase flow in a Horizontal Pipe, Flow Measurement and Instrumentation 12 (2001) 259–265
9) A.D. Okonkwo, M. Wang, B. Azzopardi, Characterization of a High Concentration Ionic Bubble Column Using Electrical Resistance Tomography, Flow Measurement and instrumentation (2012).
10) Mohammad Ramezani, Navid Mostoufi, and Mohammad Reza Mehrnia Improved Modeling of Bubble Column Reactors by Considering the Bubble Size Distribution, Ind. Eng. Chem. Res. 2012, 51, 5705−5714

11) F. Dong, Y.B. Xu, L.J. Xu, L. Hua, X.T.Qiao, Application of dual-plane ERT system and cross-correlation technique to measure gas–liquid flows in vertical upward pipe, Flow Measurement and Instrumentation 16 (2005) 191–197.

12) Ma, Y., Vlasblom, W.J., Miedema, S.A., Matousek, V., "Measurement of Density and Velocity in Hydraulic Transport using Tomography". Dredging Days 2002, Dredging without boundaries, Casablanca, Morocco, V64-V73, 22-24 October 2002.

13) Tomasz Dyakowski), Laurent F.C. Jeanmeure, Artur J. Jaworski, Applications of electrical tomography for gas–solids and liquid–solids flows — a review

14) Sharifi, M., Young, B., Electrical Resistance Tomography (ERT) applications to Chemical Engineering, Chemical Engineering Research and Design (2013).

15) Fadil Santosa and Michael Vogelius, A Back-projection Algorithm for Electrical Impedance Imaging, Vol. 50, No. 1, pp. 216-243, February 1990

16) M. Wang A. Dorward, D. Vlaev, R. MannChemical , Measurements of gas–liquid mixing in a stirred vessel using electrical resistance tomography (ERT), Engineering Journal 77 (2000) 93–98

17) F. Dong , Z.X. Jiang, X.T. Qiao, L.A. Xu, Application of electrical resistance tomography to two-phase pipe flow parameters measurement, Flow Measurement and Instrumentation 14 (2003) 183–192

18) Nigar Kantarci, Fahir Borak, Kutlu O. Ulgen, Bubble column reactors, Process Biochemistry 40 (2005) 2263–2283

19) Guadalupe Ramos Caicedo, Juan J. Prieto Marques, Monica Garcia Ruız, Jesus Guardiola Soler, A study on the behaviour of bubbles of a 2D gas-solid fluidized bed using digital image analysis, Chemical Engineering and Processing 42 (2003) 9-14.

20) Chengzhi Tang, Theodore J. Heindel, Estimating gas holdup via pressure difference measurements in a cocurrent bubble column, International Journal of Multiphase Flow 32 (2006) 850–863.

21) Maedeh Asari, Faramarz Hormozi. Effects of Surfactant on Bubble Size Distribution and Gas Hold-up in a Bubble Column, American Journal of Chemical Engineering, Vol. 1, No. 2, (2013) 50-58.

22) Fahd Mahboob Aloufi, An investigation of Gas Void Fraction and Transition Conditions for two-phase flow in an Annular gap Bubble Column, Doctoral Thesis (2011).

23) Rajamani Krishna, Jeroen W. A. de Swart, Jurg Ellenberger, Gilbert B. Martina, and Cristina Maretto, Gas Holdup in Slurry Bubble Columns: Effect of Column Diameter and Slurry Concentrations, 1997, Vol. 43, No. 2.

24) Timothy Matthew Long, An On-line Velocity Flow ProfilingSystem using Electrical Resistance Tomography,Doctoral Thesis (2006).

25) Mehran Goharian, New hardware and software design for electrical impedance tomography, Doctoral Thesis(2008).

26) Fadil Santosa and Michael Vogelius, A Backprojection Algorithm for Electrical Impedance Imaging (1990), vol. 50, no. 1, pp. 216-243.

27) A. Parvareh, M. Rahimi , A. Alizadehdakhel, A.A. Alsairafi, CFD and ERT investigations on two-phase flow regimes in vertical and horizontal tubes, International Communications in Heat and Mass Transfer 37 (2010) 304–311.

28) Jin Haibo, Lian Yicheng, Yang Suohe, Guangxiang He, Zhiwu Guo, The Parameters Measurement of Air-Water Two Phase Flow Using Electrical Resistance Tomography (ERT)Technique in A Bubble Column, Flow Measurement and Instrumentation(2012),Manuscript.

29) Dong Feng , XU Cong , Zhang Zhiqiang and Ren Shangjie Design of Parallel Electrical Resistance Tomography System for Measuring Multiphase Flow, Chinese Journal of Chemical Engineering, 20(2) 368 -379 (2012).

30) Y. G. Waghmare, C. A. Dorao, H. A. Jakobsen, F. Carl Knopf, and R. G. Rice, Bubble Size Distribution for A Bubble Column Reactor Undergoing Forced Oscillations, Ind. Eng. Chem. Res. 2009, 48, 1786–1796.

31) Mohammad Ramezani, Navid Mostoufi, and Mohammad Reza Mehrnia, Improved Modeling of Bubble Column Reactors by Considering the Bubble Size Distribution Ind. Eng. Chem. Res. 2012, 51, 5705−5714.

32) M. Bailey, C.O. Gomez, J.A. Finch , Development and Application of an Image Analysis method for wide bubble size distributions, Minerals Engineering 18 (2005) 1214–1221.

33) A Tamburrino and G Rubinacci, A new non-iterative inversion method for electrical resistance tomography, Inverse Problems 18 (2002) 1809–1829.

34) Ahmed Ali Aldalawi, Hydrodynamic Characteristic Effect of Foam Control in Three Phase Bubble Column, Master's Thesis(2007).

Appendix

Following are the tables of experimental readings from ERT for three different spargers.

			For 1ml addition of MIBC			
	reading1	readng 2	reading3			
Flowrate(LPM)	Conductivty_1(mS/cm)	Conductivty_2(mS/cm)	Conductivty_3(mS/cm)	mean	standard deviation	Gas holdup
2	0.980114	0.979819	0.979528	0.97982	0.000293002	0.0135442
3	0.972405	0.973425	0.968663	0.971498	0.00250731	0.0191838
4	0.959845	0.961427	0.960653	0.960642	0.000791061	0.0265877
5	0.946613	0.946734	0.943257	0.945535	0.001973445	0.0369816
6	0.924473	0.921959	0.92378	0.923404	0.001298492	0.0524019
			For 4ml addition of MIBC			
2	0.970599	0.969631	0.968623	0.969618	0.000988067	0.0204621
3	0.960403	0.961529	0.958687	0.960206	0.001431171	0.0268857
4	0.950204	0.930428	0.942026	0.940886	0.009937165	0.0402015
5	0.921297	0.92854	0.927584	0.925807	0.003934915	0.0507163
6	0.918124	0.91846	0.905683	0.914089	0.007281748	0.0589625
			For Tap Water			
2	0.980769	0.976504	0.975358	0.977544	0.002851387	0.0150838
3	0.963964	0.966246	0.970638	0.966949	0.003392135	0.0222792
4	0.95246	0.950006	0.950002	0.950823	0.001417974	0.0333313
5	0.938097	0.936176	0.933221	0.935831	0.002456204	0.0437141
6	0.917509	0.919227	0.916384	0.917707	0.00143177	0.0564096

Table A.1 Experimental readings and calculations for 1mm sparger

			For Water			
Flowrate(LPM)	Conductivty_1(mS/cm	Conductivty_2(mS/cm)	Conductivty_3(mS/cm)	mean	standard deviation	Gas holdup
2	0.980088	0.97915	0.979911	0.979716	0.00049838	0.0136145
3	0.968218	0.965697	0.966239	0.966718	0.001327005	0.0224369
4	0.956736	0.953139	0.948569	0.952815	0.004093149	0.0319596
5	0.932558	0.930154	0.927897	0.930203	0.002330886	0.0476397
6	0.912965	0.91097	0.908467	0.910801	0.002253776	0.0612885
mibc1			For 1ml addition of MIBC			
2	0.941837	0.942966	0.942457	0.94242	0.000565409	0.0391379
3	0.936475	0.933503	0.935443	0.93514	0.00150894	0.0441953
4	0.923165	0.92424	0.922569	0.923325	0.000846865	0.0524576
5	0.909221	0.912334	0.911998	0.911184	0.001708576	0.0610169
6	0.905414	0.905487	0.901362	0.904088	0.002360779	0.0660533
mibc4			For 4ml addition of MIBC			
2	0.928082	0.925809	0.926297	0.926729	0.001196585	0.05007
3	0.919661	0.919194	0.920214	0.91969	0.000510604	0.0550129
4	0.908135	0.910464	0.910737	0.909779	0.001429987	0.0620125
5	0.902165	0.900038	0.897468	0.89989	0.002351979	0.0690438
6	0.892567	0.889496	0.889747	0.890603	0.00170521	0.0756912

Table A.2 Experimental readings and calculations for 1.2mm sparger

			For Water			
Flowrate(LPM)	Conductivty_1(mS/cm)	Conductivty_2(mS/cm)	Conductivty_3(mS/cm)	mean	standard deviation	Gas holdup
2	0.955091	0.952187	0.949702	0.952327	0.002697213	0.03229543
3	0.929758	0.927807	0.927616	0.928394	0.0011854	0.04890485
4	0.911389	0.90974	0.909823	0.910317	0.000929018	0.06163085
5	0.891961	0.893799	0.889079	0.891613	0.002379165	0.07496646
6	0.875554	0.875911	0.875339	0.875601	0.000288923	0.08652011
			For 1ml addition of MIBC			
2	0.908997	0.908547	0.907715	0.90842	0.000650416	0.06297601
3	0.902691	0.901679	0.90174	0.902037	0.00056749	0.0675135
4	0.895001	0.891853	0.891785	0.89288	0.001837443	0.07405793
5	0.878601	0.878557	0.877189	0.878116	0.000802818	0.08469731
6	0.871638	0.870007	0.869766	0.87047	0.001018383	0.09024979
			For 4ml addition of MIBC			
2	0.897695	0.895757	0.894792	0.896081	0.001478427	0.07176502
3	0.887821	0.887452	0.887386	0.887553	0.000234429	0.07788394
4	0.876901	0.878943	0.877327	0.877724	0.001077242	0.08498129
5	0.869581	0.869261	0.866457	0.868433	0.00171873	0.09173441
6	0.860884	0.858913	0.857844	0.859214	0.001542141	0.09847906

Table A.3 Experimental readings and calculations for 1.4mm sparger